Toll-like receptor 7/8 agonists stimulate plasmacytoid dendritic cells to initiate TH17-deviated acute contact dermatitis in human subjects

Natalie Garzorz-Stark, Felix Lauffer, Linda Krause, Jenny Thomas, Anne Atenhan, Regina Franz, Sophie Roenneberg, Alexander Boehner, Manja Jargosch, Richa Batra, Nikola S. Mueller, Stefan Haak, Christina Groß, Olaf Groß, Claudia Traidl-Hoffmann, Fabian J. Theis, Carsten B. Schmidt-Weber, Tilo Biedermann, Stefanie Eyerich, Kilian Eyerich

Angaben zur Veröffentlichung / Publication details:

Garzorz-Stark, Natalie, Felix Lauffer, Linda Krause, Jenny Thomas, Anne Atenhan, Regina Franz, Sophie Roenneberg, et al. 2018. "Toll-like receptor 7/8 agonists stimulate plasmacytoid dendritic cells to initiate TH17-deviated acute contact dermatitis in human subjects." *Journal of Allergy and Clinical Immunology* 141 (4): 1320–1333.e11. https://doi.org/10.1016/j.jaci.2017.07.045.

Toll-like receptor 7/8 agonists stimulate plasmacytoid dendritic cells to initiate T_H17-deviated acute contact dermatitis in human subjects

Natalie Garzorz-Stark, MD, PhD,[a]* Felix Lauffer, MD,[a]* Linda Krause, PhD,[b] Jenny Thomas, PhD,[c] Anne Atenhan, MSc,[c] Regina Franz, MD,[a] Sophie Roenneberg, MD,[a] Alexander Boehner, MD,[a] Manja Jargosch, PhD,[c] Richa Batra, PhD,[b] Nikola S. Mueller, PhD,[b] Stefan Haak, PhD,[c] Christina Groß, PhD,[d] Olaf Groß, PhD,[d] Claudia Traidl-Hoffmann, MD,[e] Fabian J. Theis, PhD,[b,f] Carsten B. Schmidt-Weber, PhD,[c] Tilo Biedermann, MD,[a] Stefanie Eyerich, PhD,[c]‡ and Kilian Eyerich, MD, PhD[a]‡ *Munich, Neuherberg, Augsburg, and Garching, Germany*

GRAPHICAL ABSTRACT

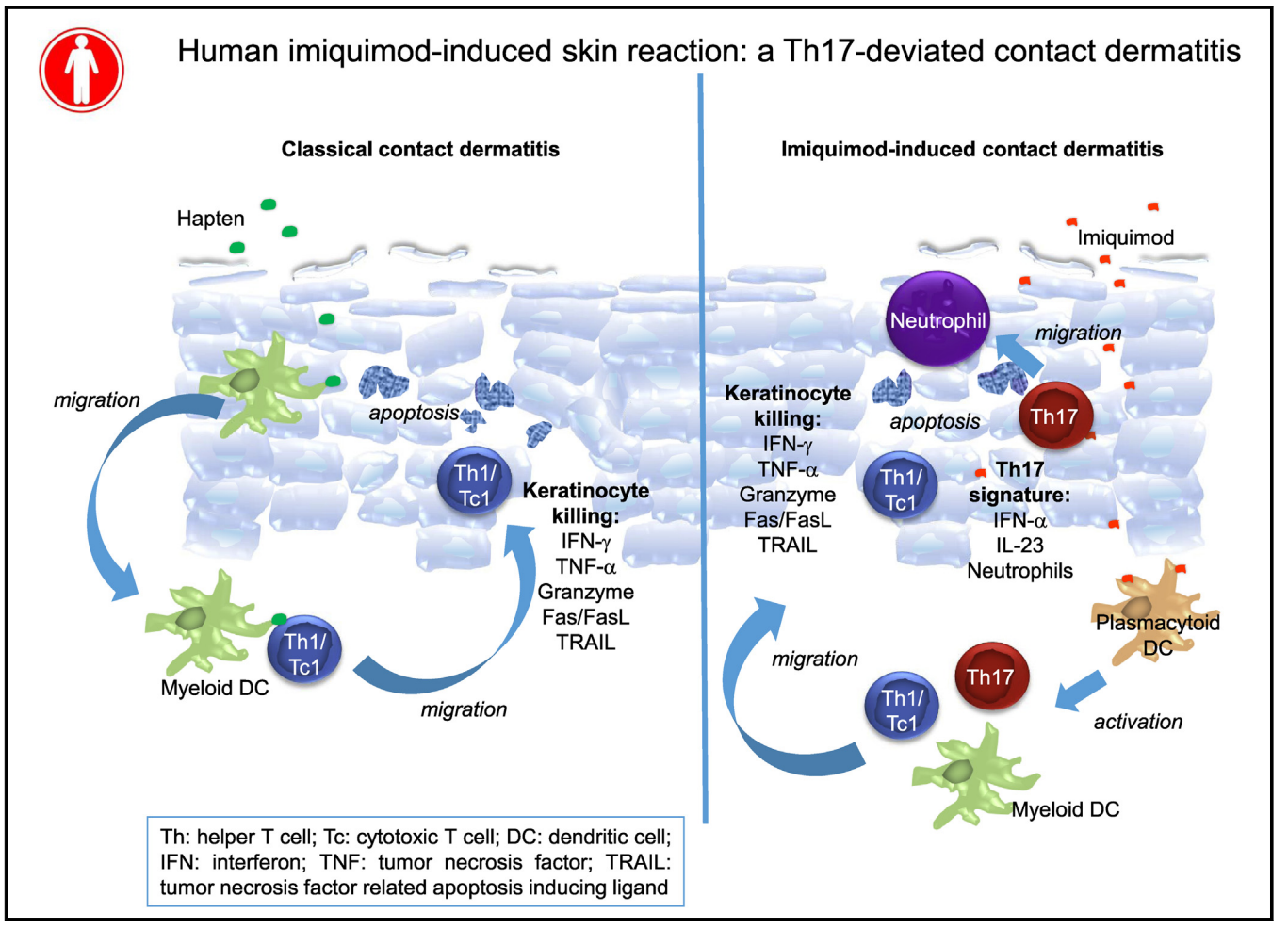

From [a]the Department of Dermatology and Allergy, Technical University of Munich; [b]the Institute of Computational Biology, Helmholtz Center Munich, Member of the German Center for Lung Research (DZL), Neuherberg; [c]ZAUM–Center of Allergy and Environment, Technical University and Helmholtz Center Munich, Member of the German Center for Lung Research (DZL), Munich; [d]the Institute for Clinical Chemistry and Pathobiochemistry, Technical University of Munich; [e]Institute of Environmental Medicine UNIKAT, Technical University and Helmholtz Center Munich, Augsburg; and [f]the Department of Mathematics, Technical University of Munich, Garching.
*These authors contributed equally to this work.
‡These authors contributed equally to this work.
Supported by the European Research Council (IMCIS 676858 and FLAMMASEC 337689), German Research Foundation (EY97/3-1), Bavarian Molecular Biosystems Research Network (BioSysNet), and Helmholtz Association ("Impuls- und Vernetzungsfonds"). L.K. is supported by the German Research Foundation (DFG) through the Graduate School of Quantitative Biosciences Munich.
Disclosure of potential conflict of interest: The authors declare that they have no relevant conflicts of interest.
Received for publication March 13, 2017; revised June 8, 2017; accepted for publication July 24, 2017.
Available online September 19, 2017.
Corresponding author: Natalie Garzorz-Stark, MD, PhD, Department of Dermatology and Allergy, Biedersteiner Strasse 29, 80802 Munich, Germany. E-mail: natalie.garzorz@tum.de.
The CrossMark symbol notifies online readers when updates have been made to the article such as errata or minor corrections
0091-6749

https://doi.org/10.1016/j.jaci.2017.07.045

Background: A standardized human model to study early pathogenic events in patients with psoriasis is missing. Activation of Toll-like receptor 7/8 by means of topical application of imiquimod is the most commonly used mouse model of psoriasis.

Objective: We sought to investigate the potential of a human imiquimod patch test model to resemble human psoriasis.

Methods: Imiquimod (Aldara 5% cream; 3M Pharmaceuticals, St Paul, Minn) was applied twice a week to the backs of volunteers (n = 18), and development of skin lesions was monitored over a period of 4 weeks. Consecutive biopsy specimens were taken for whole-genome expression analysis, histology, and T-cell isolation. Plasmacytoid dendritic cells (pDCs) were isolated from whole blood, stimulated with Toll-like receptor 7 agonist, and analyzed by means of extracellular flux analysis and real-time PCR.

Results: We demonstrate that imiquimod induces a monomorphic and self-limited inflammatory response in healthy subjects, as well as patients with psoriasis or eczema. The clinical and histologic phenotype, as well as the transcriptome, of imiquimod-induced inflammation in human skin resembles acute contact dermatitis rather than psoriasis. Nevertheless, the imiquimod model mimics the hallmarks of psoriasis. In contrast to classical contact dermatitis, in which myeloid dendritic cells sense haptens, pDCs are primary sensors of imiquimod. They respond with production of proinflammatory and T_H17-skewing cytokines, resulting in a T_H17 immune response with IL-23 as a key driver. In a proof-of-concept setting systemic treatment with ustekinumab diminished imiquimod-induced inflammation.

Conclusion: In human subjects imiquimod induces contact dermatitis with the distinctive feature that pDCs are the primary sensors, leading to an IL-23/T_H17 deviation. Despite these shortcomings, the human imiquimod model might be useful to investigate early pathogenic events and prove molecular concepts in patients with psoriasis. (J Allergy Clin Immunol 2018;141:1320-33.)

Key words: *Psoriasis, contact dermatitis, imiquimod, Aldara, plasmacytoid dendritic cell, IL-23, T_H17, cytotoxicity, Toll-like receptor, innate immunity*

Psoriasis is a noncommunicable inflammatory skin disease classified by the World Health Organization as severe. Despite enormous efforts, psoriasis is still underdiagnosed and undertreated.[1] One reason for these shortcomings is the remarkable heterogeneity in the clinical spectrum of psoriasis.[2] This heterogeneity is reflected by a high interindividual and interinvestigational variability in the transcriptome of psoriasis plaques.[3-5] By using meta-analysis approaches, downstream core genes expressed in most psoriasis plaques were proposed.[6,7] Although these downstream genes represent targets of highly efficient biologic therapies, identification of early psoriasis triggers remains difficult. At the same time, murine models only partially reflect human psoriasis.[8,9] Thus there is a high need to identify a human model that allows the standardized investigation of psoriasis plaque formation and kinetics.

Epicutaneous application of the Toll-like receptor (TLR) 7/8 agonist imiquimod is regarded as the most widely used model for psoriasis in mice.[10] Daily application of imiquimod results in a self-limited, localized, cutaneous immune response resembling histologic hallmarks of psoriasis, such as parakeratosis, acanthosis, and neutrophil microabscesses, in mice.[11] Furthermore, molecular pathways central to human psoriasis are upregulated on imiquimod stimulation, among them IFN-γ, TNF-α, and the IL-23/T_H17 axis.[12-14] Although it remains unclear what exactly drives the imiquimod-induced psoriasis-like skin inflammation in mice, dendritic cells and γδ T cells are indispensable for its development.[15,16] In human subjects incidental exacerbation of a pre-existing psoriasis plaque in a patient with psoriasis after application of imiquimod has been reported,[17] and a case series reported skin lesions partially reflecting human psoriasis after short-term application of imiquimod.[12]

The aim of this study was to comprehensively characterize imiquimod-induced inflammation in human subjects and to evaluate its potential use as a standardized human psoriasis model.

Abbreviations used
ACD: Allergic contact dermatitis
APC: Allophycocyanin
BDCA2: Blood dendritic cell antigen 2
HRP: Horseradish peroxidase
ICD: Imiquimod-induced contact dermatitis
NOS2: Nitric oxide synthase 2
pDC: Plasmacytoid dendritic cell
RT: Room temperature
TLR: Toll-like receptor

METHODS

Patients' characteristics and study design

Eighteen patients with or without a known history of psoriasis, atopic eczema, or both were included in the study (Table I). The study was conducted according to the Declaration of Helsinki and approved by the local ethics committee (5060/11). Imiquimod (Aldara 5% cream; 3M Pharmaceuticals, St Paul, Minn), 0.2 g/cm^2, was applied at days 0, 2, and 4 and subsequently twice weekly for 4 weeks in an occlusive manner on the backs of the patients. Systemic immunosuppressive treatments for 3 months or topical immunosuppressive treatment 1 week before inclusion in the study were exclusion criteria.

Punch biopsy specimens

Six-millimeter punch biopsy specimens were obtained after achievement of local anesthesia after written informed consent was obtained. Punch biopsy specimens were cut into 3 pieces: one third was paraffin embedded for histologic assessment, total RNA was isolated from the second third, and primary human cells were obtained from the last piece.

Histology

Histologic assessment was performed by 2 independent blinded pathologists. Samples were scored according to a published psoriasis and eczema score to evaluate histologic similarity to psoriasis or eczema.[12] Each criterion was evaluated separately: absence of a characteristic was scores as 0 points, mild presence of the characteristic was scored as 1 point, and full presence of the characteristic was scored as 2 points. Thus a maximum of 16 points could be achieved for the psoriasis score and a maximum of 12 points for the eczema score.

TABLE I. Patients' characteristics

Volunteer ID	Sex	Age (y)	Background	Day 4	Day 14	Day 28
1	M	35	Atopic eczema	+	++	+++
2	F	61	Healthy	++	+	+
3	F	42	Psoriasis	+++	++	+
4	F	29	Healthy	+	++	+++
5	F	45	Atopic eczema	+	+++	++
6	M	33	Psoriasis	+	+++	++/+++
7	M	46	Healthy	0		
8	F	40	Psoriasis and atopic eczema	+	+	++
9	F	51	Psoriasis	++	+++	+
10	F	53	Healthy	++	+	+
11	F	59	Psoriasis	0		
12	F	70	Atopic eczema	0		
13	F	47	Healthy	+/++	+	++
14	F	55	Healthy	+	++	+
15	M		Psoriasis	0	0	ND
16	M		Psoriasis	+	++	ND
17	F		Psoriasis	+	+	ND
18	M	23	Psoriasis and atopic eczema	++	++	ND

F, Female; *M*, male; *ND*, not determined.

Immunohistochemistry

Skin samples were fixed in 10% formalin and embedded in paraffin. Four-micrometer sections were cut and dewaxed. Staining was performed with an automated BOND system, according to the manufacturer's instructions: after rehydration and antigen retrieval in a pH 6 citrate buffer–based epitope retrieval solution (Leica, Wetzlar, Germany), sections were incubated with the mAbs rabbit anti-CD4 (Zytomed Systems, Berlin, Germany) and mouse anti-CD8 (Zytomed Systems), goat anti–IL-17 (R&D Systems, Minneapolis, Minn), rabbit anti–neutrophil elastase (Abcam, Cambridge, United Kingdom), rabbit anti-TLR7 (Abcam), Caspase 3 (Cell Signaling, Danvers, Mass), and mouse anti-CD303 (Dendritics, Lyon, France) antibodies. Secondary polymeric alkaline phosphatase–linked anti-rabbit antibody and horseradish peroxidase (HRP)–linked anti-mouse antibody (Zytomed Systems) were applied, and the complex was visualized with the substrate chromogen Fast Red or 3,3′-diaminobenzidine. For goat anti–IL-17, a goat bridge (polyclonal goat anti–IL-17 antibody; R&D Systems) was applied before application of the secondary antibody. Eventually, slides were counterstained with hematoxylin. As a negative control, primary antibodies were omitted or replaced with an irrelevant isotype-matched mAb. Positive cells for each slide were counted in 2 visual fields (×400 magnification) per condition by 2 independent investigators in a blinded manner.

Immunofluorescence

Paraffin-mounted slides were dewaxed and rehydrated in consecutive washes with Roticlear (2 changes at 10 minutes; Carl Roth, Karlsruhe, Germany), followed by isopropanol (2 changes at 5 minutes), 96% and 70% ethanol (1 change at 5 minutes, respectively) and dH_2O (1 change at 5 minutes). Antigen retrieval was performed in a pressure cooker with boiling citrate buffer (approximately 96°C) for 7 minutes, followed by a washing step with Tris buffer and a blocking step with peroxidase 3% for 15 minutes at room temperature (RT). Before applying the primary antibody (anti–inducible nitric oxide synthase antibody; Novus Biologicals, Littleton, Colo) for 1 hour at RT, and then overnight, sections were washed with Tris buffer and blocked with 10% normal goat serum and 10% normal donkey serum for 1 hour. After overnight incubation, slides were rinsed with Tris buffer and incubated with secondary antibody (488 goat-anti rabbit antibody; Life Technologies, Grand Island, NY) in the dark for 1 hour at RT. After rinsing with Tris buffer, sections were incubated in 0.1% Sudan Black B and diluted in 70% ethanol, followed by a washing step with 0.02% Tween 20 diluted in PBS and several changes of dH_2O. Before mounting the sections in Vectashield Mounting Medium (Vectro Laboratories, Burlingame, Calif), incubation with 4′-6-diamidino-2-phenylindole dihydrochloride for 2 minutes was performed. Then images in the blue (4′-6-diamidino-2-phenylindole dihydrochloride) and green (inducible nitric oxide synthase) channel of an Olympus IX73 inverted fluorescence microscope (Olympus, Center Valley, Pa) were taken.

Isolation and stimulation of lesional T cells

T cells were isolated from freshly obtained skin biopsy specimens. Samples were placed in 24-well plates precoated with α-CD3 (0.75 μg/mL α-CD3) for 1 hour containing T-cell culture medium, 0.75 μg/mL α-CD28, and 60 U/mL IL-2 and incubated at 37°C in a 5% CO_2 atmosphere. Fresh medium containing 60 U/mL IL-2 was replaced 3 times a week, and T cells that emigrated from tissue samples were expanded and harvested for flow cytometry. For protein secretion analysis, supernatants from T cells that were stimulated with plate-bound α-CD3 and soluble α-CD28 (both 0.75 μg/mL) were obtained and analyzed with the Human Cytokine 27-Plex Assay, according to the manufacturer's recommendation (Bio-Rad Laboratories, Hercules, Calif).

Isolation and stimulation of human plasmacytoid dendritic cells

Human plasmacytoid dendritic cells (pDCs) were isolated from PBMCs with the Plasmacytoid Dendritic Cell Isolation Kit II (Miltenyi Biotech, Bergisch Gladbach, Germany), leaving a pure and untouched pDC fraction. pDCs were stimulated with imiquimod, R848, and gardiquimod (100 μmol/L each) for 6 hours in RPMI supplemented with 1% human serum, 2 mmol/L glutamine, 1 mmol/L sodium pyruvate, 1% nonessential amino acids, and 1% penicillin/streptomycin.

Flow cytometry

For surface staining of T cells, the following antibodies were used: CD4 labeled with Horizon V500 or allophycocyanin (APC)–Cy7 and CD8 labeled with fluorescein isothiocyanate, Pacific Blue, or APC-Cy7 (all from BD Biosciences, San Jose, Calif). For intracellular staining, T cells were stimulated with 10 ng/mL phorbol 12-myristate 13-acetate, 1 μg/mL ionomycin, and GolgiStop (BD Biosciences), according to the manufacturer's recommendations, for 2 hours. GolgiPlug (BD Biosciences) was added for the last 4 hours of culture. Cells were fixed and permeabilized with Cytofix/Cytoperm solution (BD Biosciences) before intracellular staining with the following antibodies: IFN-γ labeled with fluorescein isothiocyanate or Horizon V450, IL-17 labeled with PE (all from BD Biosciences), and IL-22 labeled with APC or eF660 (both from eBioscience, San Diego, Calif). Cells

were analyzed with the LSRFortessa flow cytometer (BD Biosciences) and FlowJo software (TreeStar, Ashland, Ore). All gates were set according to isotype controls.

Extracellular flux analysis

Human and murine pDCs were resuspended in bicarbonate- and phenol red–free Dulbecco modified Eagle medium containing 10 mmol/L glucose, 2 mmol/L glutamine, 1 mmol/L pyruvate, and 1% FCS (Sigma-Aldrich, St Louis, Mo) and seeded in 96-well Seahorse plates (Agilent Technologies, Santa Clara, Calif) at a density of 0.15×10^6 cells per well. Cells were incubated at 37°C in a CO_2-free incubator for 1 hour before the experiment. Oxygen consumption and extracellular acidification were measured with a Seahorse XF96 Extracellular Flux Analyzer (Agilent Technologies). The compounds imiquimod, R848, and gardiquimod, as well as rotenone (2 μm) to block complex 1, were added at the indicated time points.

RT-PCR

For amplification of genes of interest, cDNA was synthesized from 500 ng of total RNA and transcribed with the High Capacity cDNA Reverse Transcript Amplification Kit (Applied Biosystems, Foster City, Calif), according to the manufacturer's protocol. Primers amplifying genes of interest were designed by using the publicly accessible Primer3 software (http://frodo.wi.mit.edu/primer3/). Real-time PCR reactions were performed in 384-well plates using the Fast Start SYBR Green Master Mix (Roche Applied Science, Penzberg, Germany), and fluorescence development was monitored with the ViiA7 Real Time PCR machine (Applied Biosystems). Expression of transcripts was normalized to expression of 18S ribosomal RNA as a housekeeping gene. Data were expressed as fold change relative to unstimulated cells as a calibrator. Relative quantification (RQ) was determined according to the following formula:

$$RQ = 2^{-\Delta\Delta Ct}.$$

Primers used were as follows: *18S* forward, GTA ACC CGT TGA ACC CCA TT; *18S* reverse, CCA TCC AAT CGG TAG TAG CG; *IL36G* forward, AG GAAGGGCCGTCTATCAATC; *IL36G* reverse, CACTGTCACTTCGTG GAACTG; *IL1B* forward, AAGCCCTTGCTGTAGTGGTG; *IL1B* reverse, GAAGCTGATGGCCCTAAACA; *IFNA* forward, CTTGACTTGCAGCT GAGCAC; *IFNA* reverse, CAGAGTCACCCATCTCAGCA; *IL23* forward, CTCAGGGACAACAGTCAGTTC; *IL23* reverse, ACAGGGCTATCAGG GAGCA; *TNFA* forward, GCCAGAGGGCTGATTAGAGA; *TNFA* reverse, TCAGCCTCTTCTCCTTCCTG; *IL6* forward, GTCAGGGGTGGTTATTG CAT; and *IL6* reverse, AGTGAGGAACAAGCCAGAGC.

Isolation of total RNA from skin

Total RNA was isolated with the miRNeasy Mini Kit (Qiagen, Hilden, Germany), according to the manufacturer's protocol. The RNA yield and quality were determined with a NanoDrop ND1000 UV-vis Spectrophotomer (Thermo Fisher, Waltham, Mass). Moreover, RNA integrity numbers were measured with the 2100 Bioanalyzer (Agilent Technologies), according to the manufacturer's protocol (Agilent RNA 6000 Nano Kit). RNA samples with RNA integrity numbers of greater than 6 were Cy3 labeled, amplified, and hybridized on SurePrint G3 Human GE 8x60K BeadChips (Agilent Technologies). Fluorescence signals were detected with the iScan microarray scanner and extracted with the Agilent Feature Extraction Software (Agilent Technologies). Transcriptomic data from samples of patients with psoriasis (n = 24) and imiquimod-induced contact dermatitis (ICD; n = 10) were previously published[3] and uploaded to the GEO database (accession no. GSE57225).

Preprocessing of whole-genome expression data

For statistical analysis of microarray data, R software (http://www.r-project.org) and the limma package from Bioconductor (http://www.bioconductor.org) were used for reading the arrays. Then QualityMetrics from Bioconductor was applied for quality control of arrays. Data were background corrected with the "normexp" method (also from limma package) and then normalized between the arrays by using the "quantile" method (from limma package). Control probes and low-expression probes with normalized signal intensities of less than 10% of the 95th percentile of the negative controls of each array were filtered out. Within-array replicates for each probe were averaged by using "avereps" (from limma package). Then "blastn" (https://blast.ncbi.nlm.nih.gov/Blast.cgi?PAGE_TYPE=BlastSearch) was used to map the 60-bp nucleotide sequences from the array (ie, probes) to the UCSC release of the human transcriptome available as RefSeqIDs. Only 100% accurate mappings were considered and saved. Of all probes, 13,430 did not match with 100% accuracy to a position of the human transcriptome. Probes mapping to 2 different RefSeq IDs were checked if they corresponded to the same gene (via Gene Symbol). The genes corresponding to the RefSeqID were received via the AnnotationDbi (from Bioconductor), which used the org.Hs.eg.db annotation Package. Eventually, 2,229 probes had to be taken out from analysis because the mapped to several genes. In total, 26,664 probes mapped with 100% accuracy to a unique gene.

Whole-genome expression visualization

Whole-genome visualization was calculated on 26,664 normalized probes for all samples by using AC-Principal component analysis (AC-PCA). This method performs dimension reduction and adjusts for confounding factors at the same time. We used the different patients as confounding factors to correct for interindividual heterogeneity. For better between-group comparison, 95% CIs per group were calculated and plotted.

Statistical modeling of gene expression data

The surrogate variable analysis from Bioconductor was used to estimate artifacts from microarray data. One surrogate variable for the data set was calculated, and we included this variable as a covariate in our regression model. By using the "lme4" package of the R software (https://cran.r-project.org/web/packages/lme4/index.html), a linear mixed-effects model was fitted to the data with the restricted maximum likelihood criterion by using 1 model per probe. Different patients were included as random effects (ie, random intercepts). Thus the gene expression level for each patient was adjusted individually. The estimated coefficients from these models are comparable with fold changes or fold inductions. *P* values for coefficients were calculated by using the mixed function from the "afex" package of R software (https://cran.r-project.org/web/packages/afex/index.html), which applies the Kenward-Roger approximation for the degrees of freedom. *P* values were adjusted for multiple testing by using Bonferroni correction. Genes were defined as significant when the adjusted *P* value was less than .05, and top hits were defined when the absolute fold change was greater than 2.5.

Gene network analysis

Pathways upregulated in ICD, allergic contact dermatitis (ACD), and psoriasis were analyzed by using the ConsensusPathDB database (http://consensuspathdb.org/). Here, by using the overrepresentation analysis tool, pathways from the pathway databases PID, Reactome, and Biocarta were selected (selection criteria: minimum overlap with input list of 2 and *P* value cutoff of .01). Among the enriched pathway-based sets, the interaction of pathways for ICD was visualized in a network. For reasons of clarity, only those pathways fulfilling the criteria of a minimum overlap of 10, the presence of at least 30% of genes within the given pathway, and a maximum gene set size of each pathway of 150 were displayed in the network. In addition, redundant pathways sharing more than 85% of genes together with another given pathway were also taken out from the network. Network data integration was performed with Cytoscape 3.4.0 software (www.cytoscape.org). Please find further Methods (Statistical analysis,

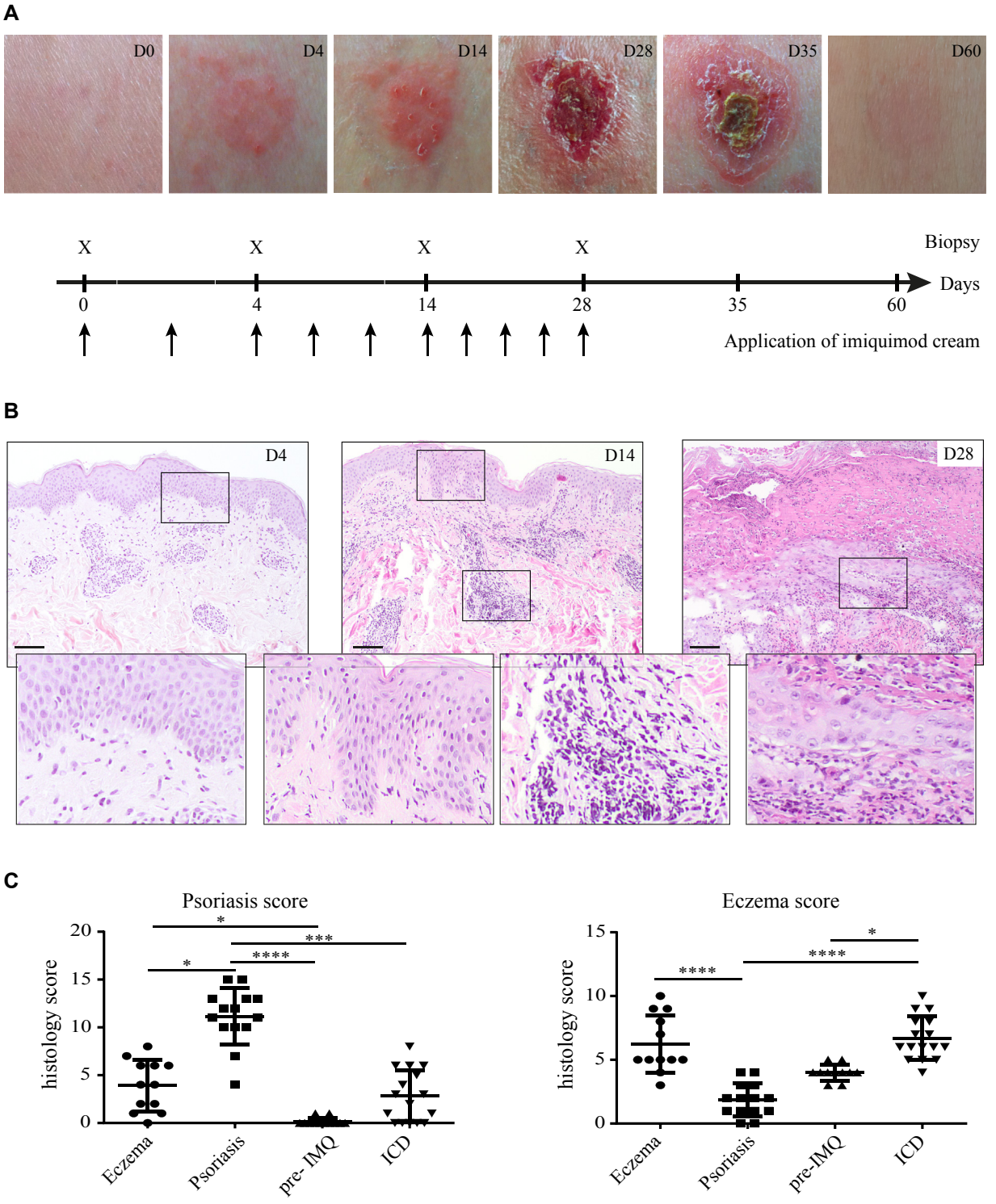

FIG 1. Topical application of imiquimod induces a self-limited acute contact dermatitis reaction. **A,** Representative clinical course of the reaction to imiquimod (ICD) in 1 patient with strong reactivity and study design. Imiquimod was applied occlusively twice weekly (scheme) until day 28, and punch biopsy specimens were obtained at days 4, 14, and 28. **B,** Hematoxylin and eosin staining of ICD lesions over time. *Bars* = 100 μm. **C,** Similarity of noninvolved skin (pre-IMQ) and ICD lesions to psoriasis and eczema, as assessed by histology scores. **P* < .05, ***P* < .01, ****P* < .001, and *****P* < .0001.

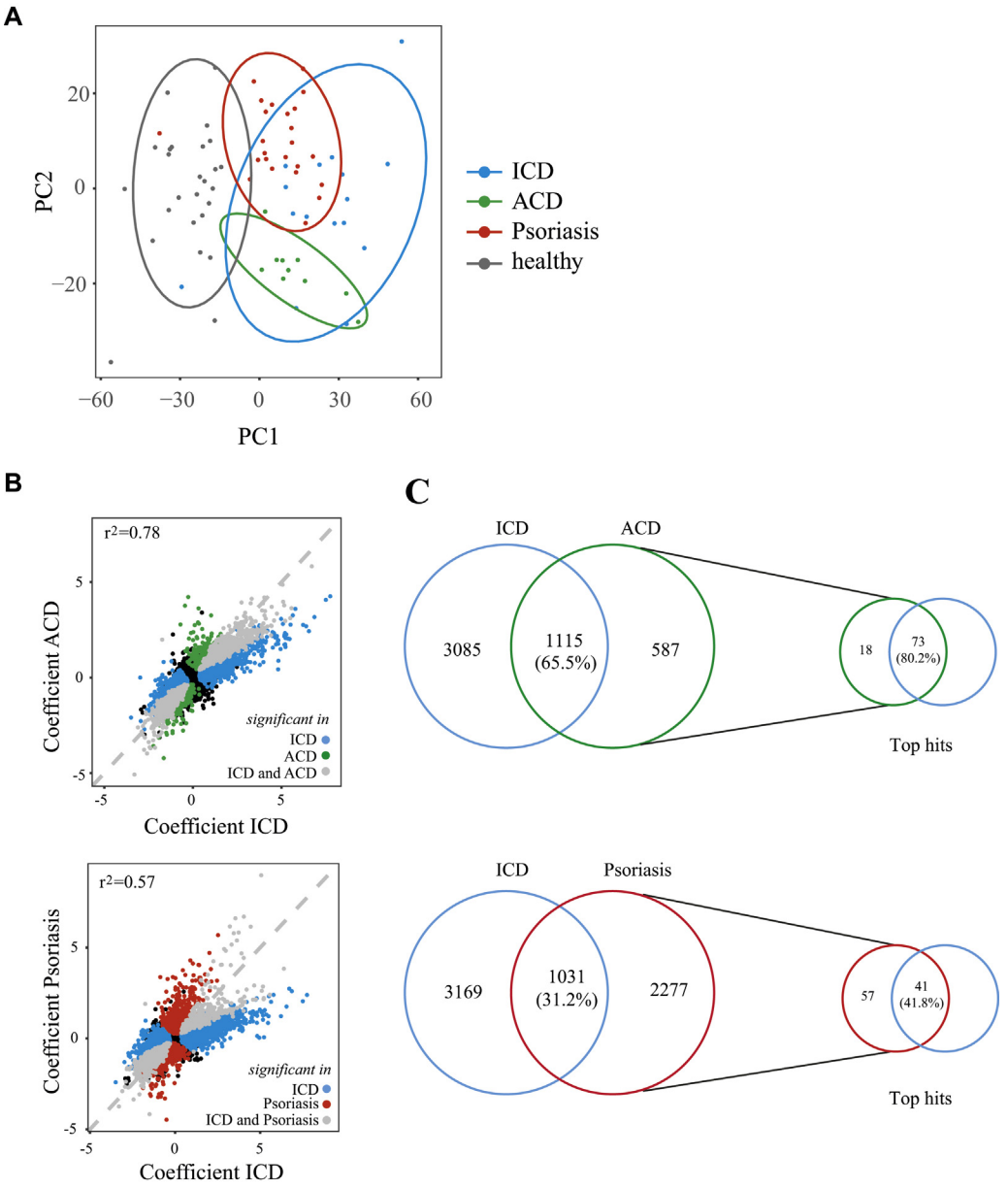

FIG 2. The ICD transcriptome closely overlaps with ACD and, to a lesser extent, with psoriasis. **A,** AC-Principal component analysis (AC-PCA) visualization of whole-genome expression analysis, including 95% CIs per group of patients with ICD (n = 16), patients with ACD (n = 10), and patients with psoriasis (n = 24) compared with noninvolved skin. *PC,* Principal component. **B,** Correlation of fold induction of all genes of ICD and ACD or of ICD and psoriasis, respectively. Gray, Genes significantly regulated in both lesions; green and red, genes significantly regulated in ACD and psoriasis lesions, respectively; blue, genes significantly regulated in patients with ICD; and black, gene that are not significantly regulated. **C,** Overlap of significantly regulated genes, as shown in Venn plots. Percentages indicate the relative number of genes regulated significantly in either patients with ACD or those with psoriasis that are also regulated significantly in patients with ICD. Smaller Venn plots indicate the overlap of top-hit genes with a $\log_2$ fold induction of greater than 2.5.

Isolation of mouse pDCs, Double-staining immuohistochemistry) in the Methods section of this article's Online Repository at www.jacionline.org.

Further statistical analysis

Statistical differences in patients with ICD versus those with psoriasis, ACD, or eczema, respectively, regarding immune histochemistry, flow cytometry, and Luminex readouts were tested by using the Kruskal-Wallis test.

Polyserial correlation was computed to show the association of clinical severity with expression levels of blood dendritic cell antigen 2 (BDCA2) or TLR7, respectively. The R package "polycor" was used. ANOVA and a *post hoc* Tukey test were applied for pairwise analysis among the severity levels by using R package stats.

RESULTS

TLR7/8 stimulation results in a self-limited contact dermatitis–like reaction in human subjects

Topical application of imiquimod (Aldara 5% cream) to nonlesional skin over a period of 28 days induced skin lesions

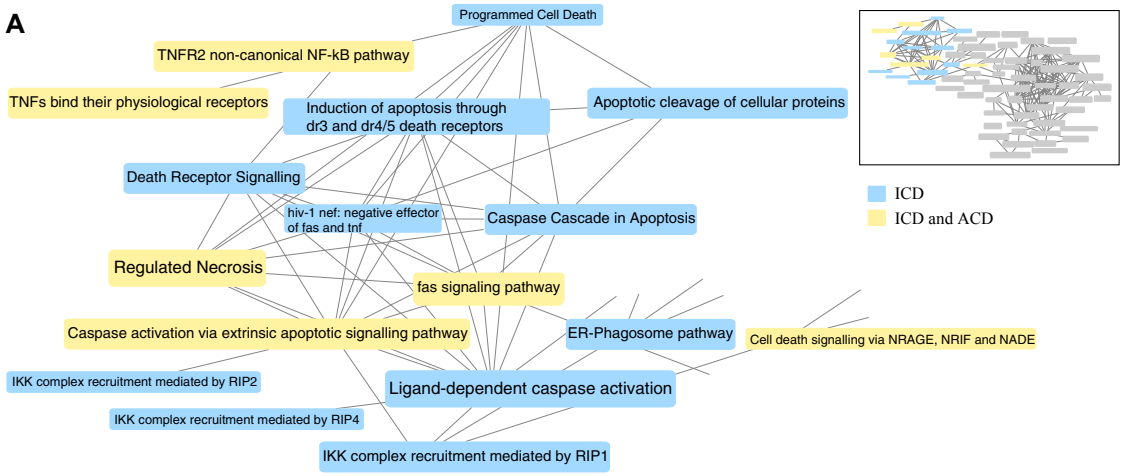
A
Programmed Cell Death
TNFR2 non-canonical NF-kB pathway
TNFs bind their physiological receptors
Induction of apoptosis through dr3 and dr4/5 death receptors
Apoptotic cleavage of cellular proteins
Death Receptor Signalling
hiv-1 nef: negative effector of fas and tnf
Caspase Cascade in Apoptosis
Regulated Necrosis
fas signaling pathway
Caspase activation via extrinsic apoptotic signalling pathway
ER-Phagosome pathway
Cell death signalling via NRAGE, NRIF and NADE
IKK complex recruitment mediated by RIP2
Ligand-dependent caspase activation
IKK complex recruitment mediated by RIP4
IKK complex recruitment mediated by RIP1
ICD
ICD and ACD

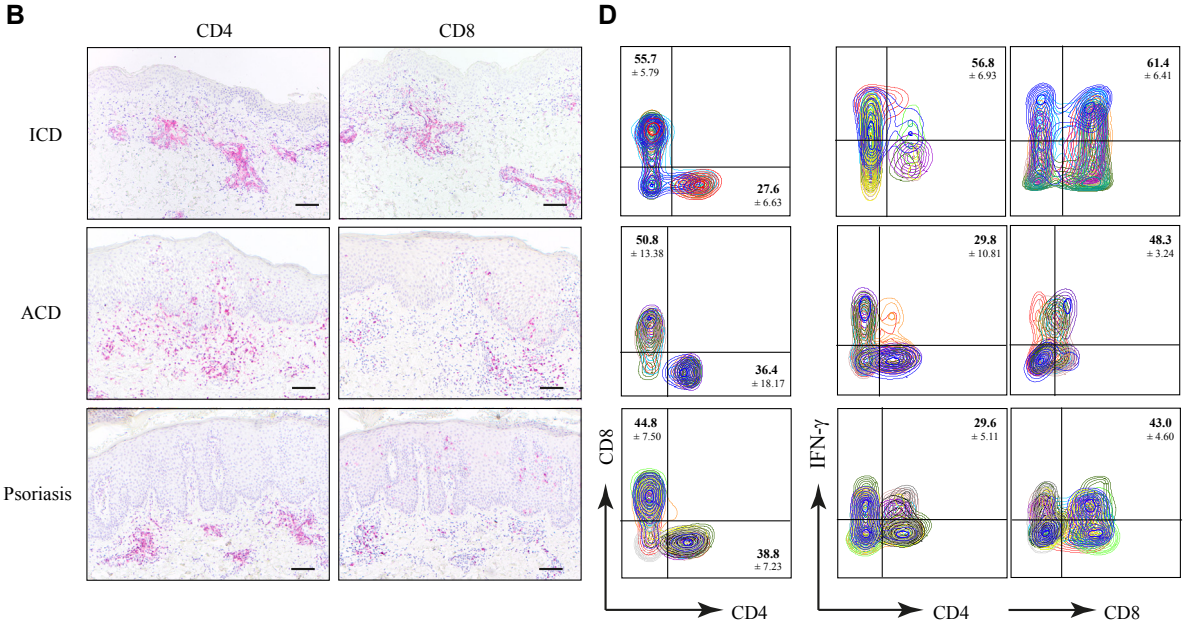
B
CD4
CD8
ICD
ACD
Psoriasis
D
55.7 ± 5.79
27.6 ± 6.63
56.8 ± 6.93
61.4 ± 6.41
50.8 ± 13.38
36.4 ± 18.17
29.8 ± 10.81
48.3 ± 3.24
44.8 ± 7.50
38.8 ± 7.23
29.6 ± 5.11
43.0 ± 4.60
CD8
IFN-γ
CD4
CD4
CD8

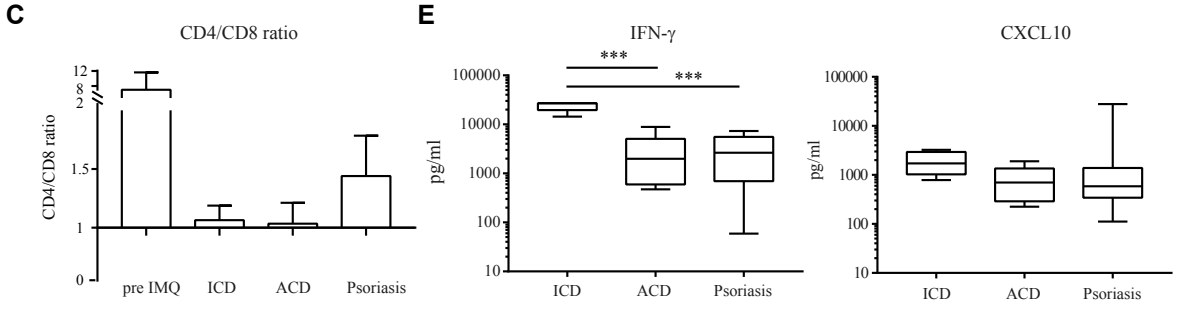
C
CD4/CD8 ratio
CD4/CD8 ratio
pre IMQ
ICD
ACD
Psoriasis
E
IFN-γ
CXCL10
pg/ml
***
***
ICD
ACD
Psoriasis

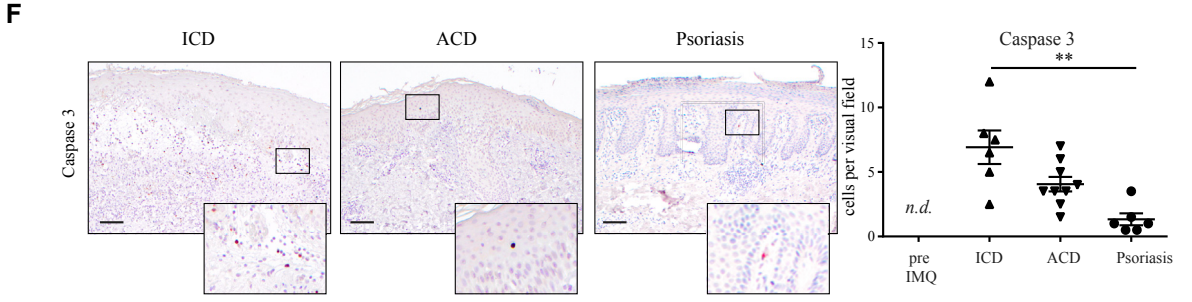
F
ICD
ACD
Psoriasis
Caspase 3
Caspase 3
**
cells per visual field
n.d.
pre IMQ
ICD
ACD
Psoriasis

resembling the clinical course of acute contact dermatitis. Initially, erythema was observed, followed by papules and induration, and finally, erosions and crusts appeared (Fig 1, *A*). The intensity of the response was heterogeneous, with 5 of 18 patients reacting only with mild erythema, 2 of 18 with erythema and papules, and 11 of 18 with the full clinical picture, including erosions (Table I). The clinical reaction to imiquimod did not augment with repetitive application in all patients. Nine of 18 patients had a maximum reaction at day 4, 3 of 18 at day 14, and 6 of 18 at day 28 (Table I). Among the healthy volunteers, patients with psoriasis, or patients with atopic eczema, neither maximum intensity nor kinetics of the reaction were related to the disease background (Table I). After withdrawal of imiquimod, lesions were self-limited within 30 days (Fig 1, *A*). Application of vehicle (Aldara cream not containing imiquimod) did not result in a clinical reaction in 1 exemplary patient (see Fig E1 in this article's Online Repository at www.jacionline.org).

Blinded histopathologic assessment of punch biopsy specimens resulted in the diagnosis of acute dermatitis in all specimens (n = 44 biopsy specimens of the 18 participants, Table I), with clear signs of spongiosis and eventually serum crusts soaked by neutrophil granulocytes (Fig 1, *B*). In 10 of 18 patients, infiltrates penetrating deeply into dermal tissue were observed at 1 or more time points (Fig 1, *B*). Hallmarks of psoriasis, such as regular acanthosis, parakeratosis, loss of stratum granulosum, and microabscesses, were absent in all samples. To quantify the similarity of the ICD (n = 16) to both psoriasis and eczema, respectively, histopathologic scores[12] were determined for biopsy sections of patients with psoriasis (n = 14), patients with eczema (n = 12), and study participants before application of imiquimod (n = 12; Fig 1, *C*). Results confirmed a low similarity of ICD with psoriasis in the psoriasis score (ICD, 2.81 ± 0.68; psoriasis, 11.14 ± 0.79) and higher eczema scores for ICD (ICD, 6.69 ± 0.43; psoriasis, 1.86 ± 0.35).

Transcriptome of human imiquimod-induced dermatitis closely overlaps with contact dermatitis but also shares pathways with psoriasis

Whole-genome expression analysis of lesional skin (n = 16) was compared with skin of patients with psoriasis (n = 24), patients with ACD to nickel (n = 10), and patients with eczema (n = 15) and noninvolved skin (n = 26) to investigate ICD in a heuristic global approach. As a first step, dimension reduction simultaneously adjusting for the confounding variation from patient heterogeneity was performed (AC-PCA).[18] A close overlap of ICD reactions with both ACD and psoriasis reactions compared with noninvolved skin was observed when examining the 95% CIs per group (Fig 2, *A*).

For a more detailed insight into the similarity of ICD and psoriasis, ACD, or eczema, significantly regulated genes were compared. The ICD and ACD transcriptomes showed a strong correlation of all significantly regulated genes ($r = 0.78$). In comparison, ICD and psoriasis ($r = 0.57$), as well as ICD and eczema ($r = 0.56$), correlated less (Fig 2, *B*, and see Fig E2, *A*, in this article's Online Repository at www.jacionline.org). Furthermore, 65% of all significantly regulated genes in patients with ACD were also regulated in patients with ICD, whereas 31.2% of the psoriasis and 37.1% of the eczema genes were also regulated in patients with ICD (Fig 2, *C*, and see Fig E2, *B*). Among the top-hit genes with a $\log_2$ fold induction of greater than 2.5, the overlap was higher, with 80.2%, 41.8%, and 64.3% for the ACD, psoriasis, and eczema transcriptomes, respectively (Fig 2, *C*, and see Fig E2, *B*).

ICD is dominated by a cytotoxic T-cell response: Similarities to ACD but not psoriasis

Gene network analyses of common and unique pathways were performed to investigate the similarities and differences of ICD (n = 16) compared with psoriasis (n = 24) or ACD (n = 10) in a qualitative manner (see Fig E3 and Table E1). ICD and ACD showed a strong correlation in regulated genes related to apoptosis ($r = 0.89$). The correlation of ICD and psoriasis was less remarkable ($r = 0.61$; Fig 3, *A*, and see Fig E4 in this article's Online Repository at www.jacionline.org).

In line with the latter observation, immunohistochemical staining showed that more cytotoxic $CD8^+$ T cells infiltrated ICD lesions (89.3 ± 12.58, n = 16) than psoriasis lesions (42.3 ± 7.97, n = 11; $P = .0008$). No significant difference was found comparing the number of $CD8^+$ T cells infiltrating patients with ICD and those with ACD (64.8 ± 12.05, n = 6; Fig 3, *B*, and see Fig E5 in this article's Online Repository at www.jacionline.org). Accordingly, the CD4/CD8 T-cell ratio was lower in patients with ICD compared with those with ACD, psoriasis, and eczema (Fig 3, *C*, and see Fig E2, *B*).

Isolation of T cells from lesional skin confirmed a higher frequency of $CD8^+$ than $CD4^+$ T cells in patients with ICD (55.7% ± 5.79% vs 27.6% ± 6.63%, n = 10) compared with

FIG 3. Both ICD and ACD reactions are dominated by immune-mediated cytotoxicity. **A,** Comparative transcriptomic analysis of lesional ICD (n = 16), ACD (n = 10), and psoriasis (n = 24) revealed pathways related to apoptosis in both patients with ICD and those with ACD but not in patients with psoriasis. Outtake of the whole network is indicated at right. Blue, Pathways regulated exclusively in patients with ICD; yellow, pathways regulated in patients with ICD and those with ACD. Font size indicates the relative percentage of regulated genes within the pathway (small, 0% to 40% of all genes; medium, 40% to 60%; large, >60%). *ER*, Endoplasmic reticulum; *IKK*, IκB kinase; *NADE*, NH(3)-dependent NAD(+) synthetase; *NRAGE*, melanoma-associated antigen D1; *NRIF*, neurotrophin receptor interacting factor; *TNFR2*, tumor necrosis factor receptor 2. **B,** Representative immunohistochemical staining of lesional ICD, ACD, and psoriasis for CD4 *(left column)* and CD8 *(right column)*. *Bars* = 100 μm. **C,** CD4/CD8 ratio for noninvolved skin (pre-IMQ) and skin of patients with ICD, ACD, and psoriasis, as calculated from mean numbers of cells per visual field in immunohistochemical staining. Shown are means ± SEMs. **D,** Flow cytometric analysis of T cells isolated from ICD, ACD, or psoriasis lesions. Shown is a merge of all patients, with each color representing 1 patient. *Left column*, Surface staining of CD4 and CD8; *middle* and *right columns*, combined surface staining of CD4 (middle) or CD8 *(right column)* and intracellular cytokine staining for IFN-γ. Numbers in each quadrant provide relative percentage. **E,** IFN-γ or CXCL10 secretion into supernatants of primary T cells derived from ICD, ACD, or psoriasis lesions 72 hours after T-cell receptor stimulation. *Box plots* indicate medians and 95% CIs. **F,** Representative immunohistochemical staining for caspase-3 in 1 ICD, ACD, or psoriasis lesion and quantitative numbers of caspase 3–positive cells per visual field. *Bars* = 100 μm. $*P < .05$, $**P < .01$, and $***P < .001$.

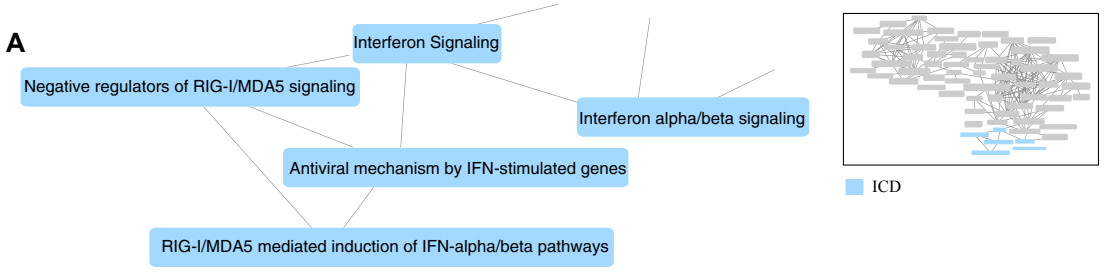
A
Interferon Signaling
Negative regulators of RIG-I/MDA5 signaling
Interferon alpha/beta signaling
Antiviral mechanism by IFN-stimulated genes
RIG-I/MDA5 mediated induction of IFN-alpha/beta pathways
ICD

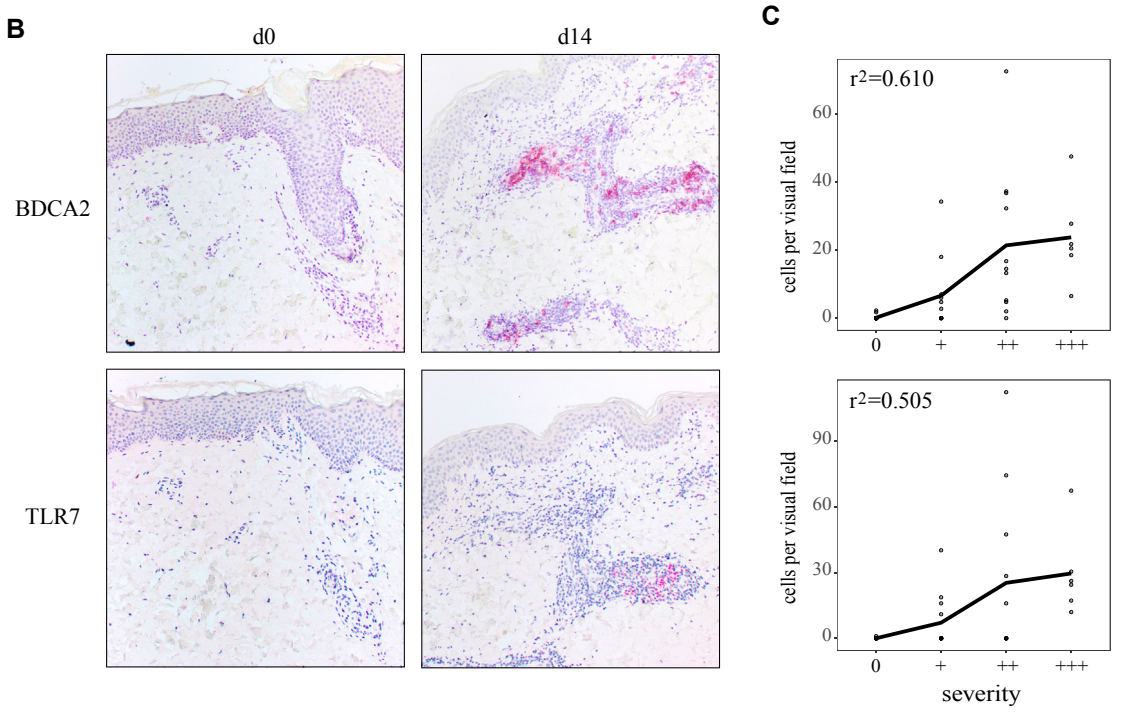
B
d0
d14
BDCA2
TLR7
C
r²=0.610
cells per visual field
0
+
++
+++
r²=0.505
severity

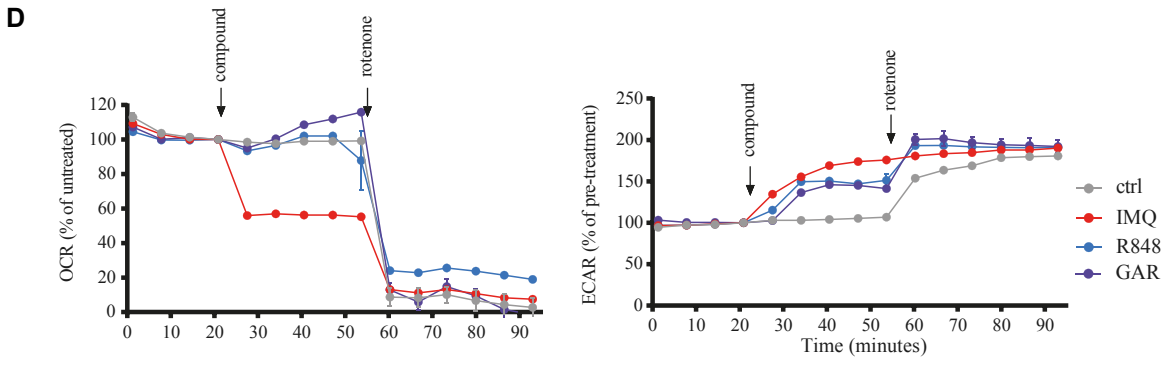
D
compound
rotenone
OCR (% of untreated)
ECAR (% of pre-treatment)
Time (minutes)
ctrl
IMQ
R848
GAR

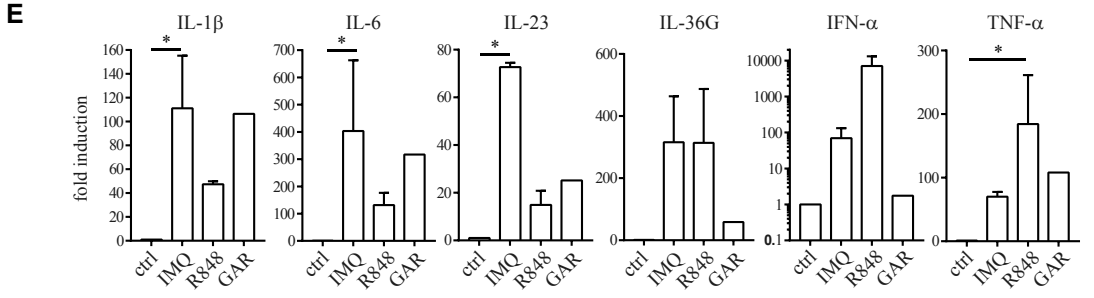
E
IL-1β
IL-6
IL-23
IL-36G
IFN-α
TNF-α
fold induction
ctrl
IMQ
R848
GAR

those with psoriasis (44.8% ± 7.5% vs 38.8% ± 7.23%, n = 14; Fig 3, *D*). Differences from patients with ACD were less pronounced (50.8% ± 13.38% vs 36.4% ± 18.17%, n = 7). The CD4/CD8 T-cell ratio was lower in cells investigated *in vitro* compared with those in immunohistochemical staining. A substantial population of both $CD4^+$ and $CD8^+$ T cells secreted IFN-γ, as investigated by using intracellular cytokine staining (Fig 3, *D*). Although a substantial frequency of $CD8^+$ and $CD4^+$ T cells in patients with ICD produced IFN-γ (61.4% ± 6.41% vs 56.8% ± 6.93%, n = 10), frequencies of IFN-γ^+ cells were comparable in patients with psoriasis and those with ACD ($CD8^+$ = 43.0% ± 4.60% [n = 14] and $CD4^+$ = 29.6% ± 5.11% and $CD8^+$ = 48.3% ± 3.24% and $CD4^+$ = 29.8% ± 10.81% [n = 7], respectively). However, T cells isolated from patients with ICD secreted more IFN-γ on T-cell receptor stimulation (23,618 ± 1,487 pg/mL; n = 10) than T cells from patients with psoriasis (3,167 ± 774 pg/mL; n = 12) or patients with ACD (2,988 ± 1,062 pg/mL; n = 8) (Fig 3, *E*). No significant differences in secretion of CXCL10 was detectable (Fig 3, *E*).

The level of caspase 3–positive cells was quantified *in situ* to assess the functional consequence of this cytotoxic T-cell infiltrate in patients with ICD (Fig 3, *F*). Samples from patients with ICD contained more caspase 3–positive cells (6.9 ± 1.30 per visual field, n = 6) than those from patients with ACD (4.1 ± 0.57, n = 9). This is consistent with the gene network analysis revealing more programmed cell death and caspase-related pathways in patients with ICD than those with ACD. Caspase 3–positive cells were very low in patients with psoriasis (1.3 ± 0.46, n = 6).

In contrast to ACD reactions, pDCs are the primary responder cells in patients with ICD

We next assessed whether the primary target of imiquimod would explain differences from ACD. Gene network analysis of pathways unique for ICD identified interferon signaling to be regulated exclusively in patients with ICD (Fig 4, *A*, and see Fig E3). Fifty-three of 73 genes related to the signaling pathway IFN-α/β signaling were significantly regulated in patients with ICD, whereas only 12 of 73 genes were regulated in patients with psoriasis and 13 of 73 genes in patients with ACD (see Fig E6 in this article's Online Repository at www.jacionline.org). Because TLR7 and TLR8 are highly expressed by pDCs and pDCs are the main producers of IFN-α, pDCs were investigated in patients with ICD reactions.

In situ staining of pDCs with the marker BDCA2 demonstrated higher numbers of pDCs in patients with ICD (18.0 ± 3.69, n = 16) than in patients with psoriasis (5.2 ± 2.13, n = 12) or those with ACD (14.8 ± 3.49, n = 6; Fig 4, *B*, and see Fig E7 in this article's Online Repository at www.jacionline.org). Levels of the main receptor for imiquimod, TLR7, were increased during the clinical course of the ICD reaction compared with those in noninvolved skin (Fig 4, *B*). Likewise, the number of $BDCA2^+$ cells increased, pointing to an influx of pDCs and upregulation of the receptor on ligation *in situ* (Fig 4, *B*). Immunohistochemical double staining identified numerous $BDCA2^+TLR7^+$ cells (see Fig E7). The severity of the clinical reaction correlated with the number of $BDCA2^+$ cells (r^2 = 0.610) and TLR7 density (r^2 = 0.505), indicating a functional role for pDCs in patients with ICD (Fig 4, *C*).

Stimulation of pDCs with imiquimod resulted in a decrease in mitochondrial respiration and an increase in glycolytic extracellular acidification in extracellular flux analysis (Fig 4, *D*). Of note, this was not observed on pDC stimulation with further TLR7/8 agonists, such as R848 or gardiquimod, confirming a TLR7/8-independent metabolic reprogramming activating the NLRP3 inflammasome by imiquimod.[19] This reprogramming by imiquimod was observed in both human (Fig 4, *D*) and murine (see Fig E8 in this article's Online Repository at www.jacionline.org) pDCs, indicating a shared cellular mechanism between mouse imiquimod-induced psoriasis-like reactions and ICD. Ligation of TLR7/8 by imiquimod, R848, and gardiquimod stimulated pDCs to produce proinflammatory and T_H17-associated molecules, among them IL-1β (mean fold induction by imiquimod/R848/gardiquimod, 111/47/106), IL-6 (403/132/317), IL-23 (73/15/25), IL-36G (316/314/59), IFN-γ (69/7021/2), TNF-α (70/184/108), and CXCL8 (1885/246/131), compared with nonstimulated control pDCs (n = 3 different donors; Fig 4, *E*).

pDCs induce the IL-23/T_H17 axis and influx of neutrophils in patients with ICD

Because pDCs are involved in the early pathogenesis of psoriasis, we next investigated the molecular overlap of ICD and psoriasis. Gene network analysis identified IL-23–mediated signaling events as a key pathway upregulated in both patients with ICD and those with psoriasis (Fig 5, *A*, and see Fig E3). Twenty-one of 42 genes related to the IL-23 signaling pathway were significantly regulated in patients with ICD. IL-23A was significantly upregulated in both patients with ICD and those with psoriasis but not in patients with ACD (Fig 5, *B*, and see Fig E9 in this article's Online Repository at www.jacionline.org). IL-23 is a key driver of T_H17 immunity. Accordingly, IL-17^+ cells were more frequent in patients with ICD (10.3 ± 1.78, n = 16) than in patients with ACD (4.0 ± 0.83, n = 8) and comparable with numbers in patients with psoriasis

FIG 4. pDCs are the primary sensory cells in patients with ICD. **A,** Comparative transcriptomic analysis of patients with lesional ICD (n = 16), ACD (n = 10), and psoriasis (n = 24) revealed unique pathways for ICD (blue) in the type 1 interferon-signaling cascade. Outtake of the whole network shown in frame and in Fig E3. *RIG-I/MDA5,* Retinoic acid inducible gene I/melanoma differentiation antigen 5. **B,** The number of $BDCA2^+$ cells and staining intensity of TLR7 increased during the course of the reaction, as shown in 1 representative patient at day 0 *(left)* and day 14 *(middle).* **C,** Number of $BDCA2^+$ cells (r^2 = 0.610) and staining intensity for TLR7 (r^2 = 0.505) *in situ* correlated with the clinical severity of the reaction. **D,** Oxygen consumption rate (*OCR*; *left graph*) and extracellular acidification *(ECAR)* of primary human pDCs stimulated with imiquimod *(IMQ),* R848, or gardiquimod *(GAR)* over time compared with values in unstimulated pDCs. *Arrows* indicate addition of compound or rotenone application. **E,** Real-time PCR analysis of primary human pDCs stimulated with imiquimod *(IMQ),* R848, or gardiquimod *(GAR)* for 6 hours. Shown is the fold induction compared with unstimulated pDCs.

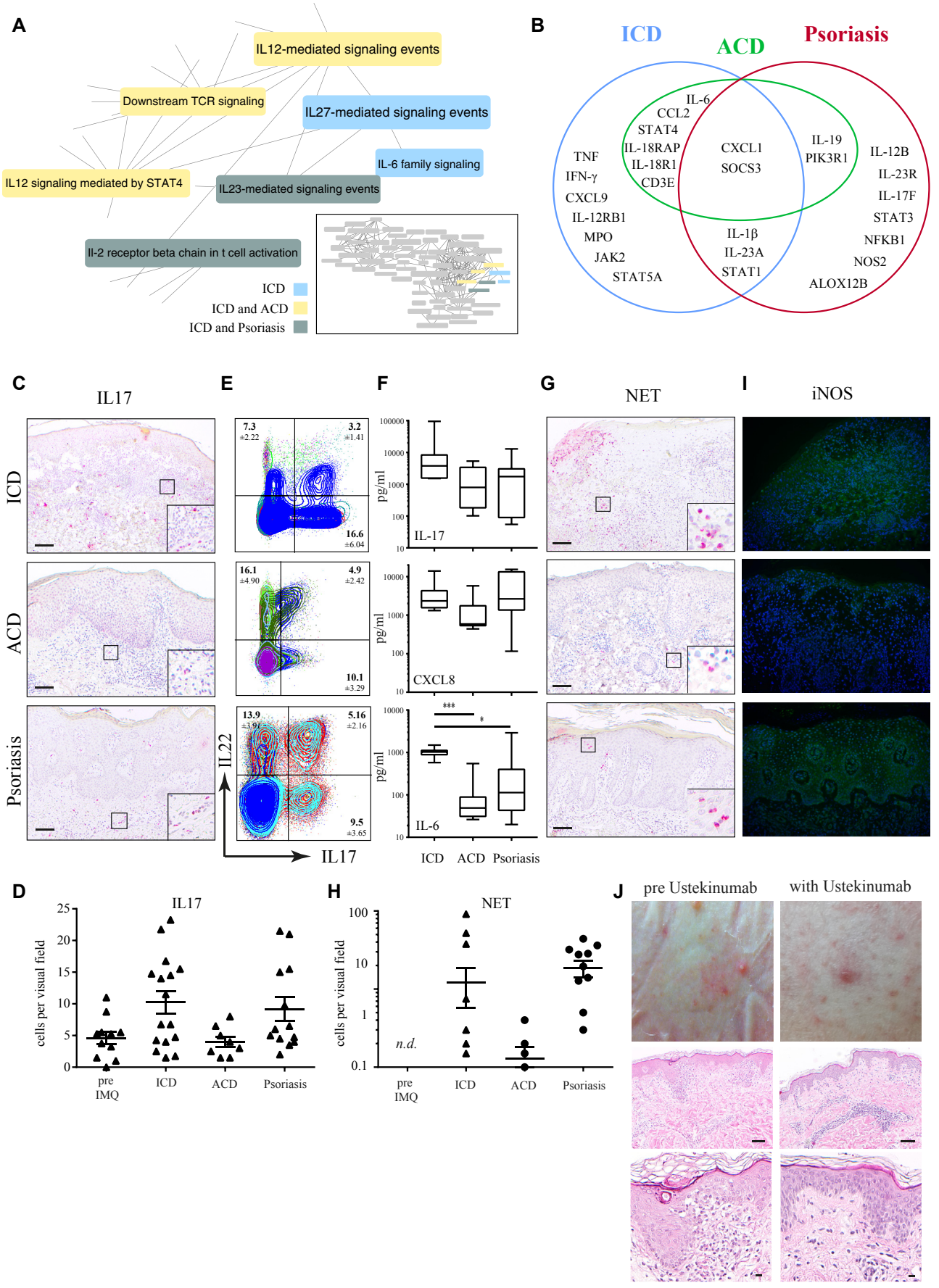
A
IL12-mediated signaling events
Downstream TCR signaling
IL27-mediated signaling events
IL-6 family signaling
IL12 signaling mediated by STAT4
IL23-mediated signaling events
Il-2 receptor beta chain in t cell activation
ICD
ICD and ACD
ICD and Psoriasis
B
ICD
ACD
Psoriasis
IL-6
CCL2
STAT4
IL-18RAP
IL-18R1
CD3E
CXCL1
SOCS3
IL-19
PIK3R1
TNF
IFN-γ
CXCL9
IL-12RB1
MPO
JAK2
STAT5A
IL-1β
IL-23A
STAT1
IL-12B
IL-23R
IL-17F
STAT3
NFKB1
NOS2
ALOX12B
C
IL17
ICD
ACD
Psoriasis
E
7.3 ±2.22
3.2 ±1.41
16.6 ±6.04
16.1 ±4.90
4.9 ±2.42
10.1 ±3.29
13.9 ±3.91
5.16 ±2.16
9.5 ±3.65
IL22
IL17
F
pg/ml
IL-17
CXCL8
IL-6
***
*
ICD ACD Psoriasis
G
NET
I
iNOS
D
IL17
cells per visual field
pre IMQ
ICD
ACD
Psoriasis
H
NET
n.d.
J
pre Ustekinumab
with Ustekinumab

in situ (9.2 ± 1.88, n = 13; Fig 5, *C* and *D*). Immunohistochemical findings were confirmed *in vitro*. Of T cells isolated from ICD lesions (n = 10), 16.6% ± 6.04% produced IL-17 in patients with ICD compared with those with psoriasis (9.5% ± 3.65%) and those with ACD (10.1% ± 3.29%). IL-22$^+$ cells were reduced in patients with ICD (7.3% ± 2.22%) compared with those in patients with ACD (16.1% ± 4.90%) and patients with psoriasis (13.9% ± 3.91%; Fig 5, *E*). Likewise, ICD-derived T cells secreted high amounts of IL-17 after T-cell receptor stimulation *in vitro* (13,408 ± 9,139 pg/mL; n = 10) compared with patients with ACD (1,612 ± 704 pg/mL; n = 8) and even patients with psoriasis (2,677 ± 1,057 pg/mL; n = 12; Fig 5, *F*).

In addition to IL-17, T cells derived from patients with ICD also secreted significantly higher amounts of IL-6 (1012 ± 80 pg/mL; n = 10), a cytokine involved in T_H17 cell differentiation, than in T cells derived from patients with ACD (113 ± 63 pg/mL, n = 8; $P = .0007$) or psoriasis (433 ± 236 pg/mL, n = 12; $P = .015$) *in vitro*. CXCL8, a chemokine recruiting neutrophil granulocytes, was highly secreted by both ICD-derived (3743 ± 1221 pg/mL, n = 10) and psoriasis-derived (6249 ± 1753 pg/mL, n = 12) T cells. CXCL8 secretion by ACD-derived T cells was lower (1494 ± 638 pg/mL, n = 8; Fig 5, *F*). Consequently, a higher number of neutrophil granulocytes was detected in lesions from patients with ICD (12.2 ± 6.72, n = 15) and those with psoriasis (18.6 ± 4.35, n = 12) than in patients with ACD (1.3 ± 0.53, n = 7) *in situ* (Fig 5, *G* and *H*).

Beyond similarities concerning the immune cell profile, ICD and psoriasis shared induction of nitric oxide synthase 2 (NOS2) in lesional skin. NOS2 is a valid metabolic marker of psoriasis.[3] In contrast, NOS2 was almost absent in patients with ACD (Fig 5, *I*).

As a proof of concept, an influence of blocking IL-23 on ICD was investigated. One patient with severe psoriasis had moderate ICD 14 days after application of imiquimod, with typical development of papules and a histologic correlate in spongiosis with epidermal dyskeratoses and a perivascular immune infiltration (Fig 5, *J*). Subsequently, psoriasis treatment with ustekinumab, an IL-12p40 antibody that neutralizes the effects of IL-23, was initiated. Six weeks after initiation, imiquimod was again applied to the patient in an identical setting. This time, the ICD reaction in this 1 patient was less remarkable clinically; histopathology described a perivascular immune infiltration and an unaltered epidermis (Fig 5, *J*).

DISCUSSION

A standardized human model of psoriasis is missing. In this study we evaluated a commonly used mouse model of psoriasis for its possible value in the human setting. Epicutaneous application of imiquimod stimulated pDCs through TLR7/8 ligation *in vivo* to induce an acute cutaneous inflammation mimicking contact dermatitis and pseudolymphoma. Despite a clinical and histologic phenotype, the human imiquimod model allows insight into the pathogenesis of psoriasis.

The principle to patch small molecules or antigens epicutaneously as a model for inflammatory skin diseases is established in patients with atopic eczema, the most common noncommunicable inflammatory skin disease other than psoriasis. Here, the so-called atopy patch test is a recognized model of early lesions.[20,21] Despite its limitations, the hypothesis of an immune evolution in patients with atopic eczema from a pure T_H2 response to a mixed immune infiltration (previously called "molecular switch") was developed from studies using the atopy patch test.[22] Thus a standardized human patch test model is of worth to investigate the pathogenesis of a complex disease *in vivo*, even if not all aspects of the disease are covered.

Application of imiquimod over a period of 28 days induced the clinical picture of acute contact dermatitis; over time, erosions developed. After imiquimod withdrawal, the lesions were self-limited, without showing clinical signs of psoriasis. In line with the clinical course, histologic analysis revealed dyskeratosis, spongiosis, and destruction of the epidermis with serum crusts containing neutrophil granulocytes. Severe reactions were accompanied by deep dermal lymphocytic infiltrates. Early lesions were similar to those reported in a case series that investigated cutaneous inflammation after tape stripping and short-term application of imiquimod.[12]

The reaction to imiquimod showed interindividual differences regarding kinetics and quantity, but it was monomorphic and independent of the disease background. Thus it seems unlikely that patients with psoriasis are generally prone to have psoriasis on stimulation with imiquimod, as observed in single cases.[17,23] Furthermore, although the formulation of Aldara cream is proinflammatory beyond TLR7/8,[24] the reaction observed in our study was dependent on imiquimod because a vehicle control did not induce inflammation.

In line with the clinical and histologic phenotype, we demonstrate that the transcriptome of imiquimod-induced inflammation largely resembles ACD rather than psoriasis.

FIG 5. ICD is a T_H17-deviated contact dermatitis. **A,** Comparative transcriptomic analysis of lesional ICD (n = 16), ACD (n = 10), and psoriasis (n = 24) revealed the IL-23 pathway is shared by patients with ICD and those with psoriasis (dark gray). Outtake of the whole network is indicated at right. Font size indicates the relative percentage of regulated genes within the pathway (smaller, 40% to 60%; larger, >60%). **B,** Genes of the IL-23 pathway significantly regulated in patients with ICD, psoriasis, and/or ACD. **C,** Representative immunohistochemical staining of ICD, ACD, and psoriasis for IL-17. **D,** Quantitative analysis of IL-17$^+$ cells in immunohistochemical staining. Shown are means ± SEMs, with each *symbol* representing 1 sample. **E,** Flow cytometric analysis of T cells isolated from ICD, ACD, or psoriasis lesions, respectively. Shown is a merge of all patients, with each color representing 1 patient. Intracellular cytokine staining for IL-17 *(x-axis)* and IL-22 *(y-axis)* is shown. Numbers in each quadrant show relative percentages. **F,** IL-17, CXCL8, or IL-6 secretion into supernatants of primary T cells derived from ICD, ACD, or psoriasis lesions 72 hours after T-cell receptor stimulation. *Box plots* indicate medians and 95% CIs. **G,** Representative immunohistochemical staining of ICD, ACD, and psoriasis lesions for neutrophil elastase *(NET)*. **H,** Quantitative analysis of NET$^+$ cells in immunohistochemical staining. Shown are means ± SEMs, and each *symbol* represents 1 sample. *n.d.*, Not determined. **I,** Immunofluorescence staining of 1 representative ICD, ACD, and psoriasis lesion. *iNOS*, Inducible nitric oxide synthase. **J,** Clinical and histologic reaction after 9 days of imiquimod application in 1 patient with psoriasis before and after 6 weeks of ustekinumab therapy.

This includes major pathogenic hallmarks of ACD, such as IFN-α signaling, upregulation of cytotoxic granules, and apoptosis.[25,26]

Increasing evidence suggests that ACD is initiated by the innate immune system sensing danger.[27] Common antigens eliciting ACD mimic infection by stimulating pattern recognition receptors, such as TLRs.[28,29] Also, in patients with psoriasis, pattern recognition receptors and sensing danger seem to be pivotal for early pathogenesis. Antimicrobial peptides, chemokines, and complexes of self-DNA or microbial DNA orchestrate the stimulation of pDCs to secrete IFN-α and a subsequent T_H17 immune response.[2,30,31] Our study confirms that the number of $TLR7^+$ pDCs increases on stimulation with imiquimod. pDCs respond with stress signals and production of proinflammatory cytokines that ultimately lead to both cell growth arrest[19] and a T_H17 immune response. Of note, NOS2 is upregulated also in the course of imiquimod-induced inflammation. NOS2 is a specific marker for psoriasis that is typically not expressed in patients with all subtypes of eczema, including ACD.[3,32] Taken together, our study supports the concept that imiquimod induces an acute contact dermatitis response with the special trait that pDCs act as primary sensors, and this trait is shared with human psoriasis.

A second important difference of classical contact dermatitis reactions and imiquimod-induced inflammation is the major role of IL-23. In several genetically modified mouse models, diminished inflammatory responses to imiquimod could be restored by injection of IL-23, among them IL-17 knockout,[33] ablation of nociceptive sensory neurons,[34] and knockout of distinct subsets of dendritic cells.[15,16] Our study demonstrates that IL-23 is also a key driver of human imiquimod-induced inflammation. This is supported by a proof-of-concept experiment of 1 patient with psoriasis who showed a diminished response to imiquimod during therapy with ustekinumab, an antibody blocking IL-12p40 that is approved to treat moderate-to-severe psoriasis.[35] Of note, biologic therapies inhibiting selectively IL-23 show overwhelming efficacy in treating psoriasis in clinical trials.[36,37]

In summary, triggering TLR7/8 elicits a self-limited contact dermatitis reaction mediated by pDCs and IL-23 in human subjects. There is a discrepancy between clinical and histologic phenotype on the one hand and the molecular signature and invading immune cells on the other hand in this model. Despite these limitations, the human imiquimod patch test model can be used to investigate early pathogenic events in patients with psoriasis.

We thank Jana Sänger for excellent technical support. This study was performed with samples from the biobank Biederstein of the Technical University of Munich.

Key messages

- **Epicutaneous application of imiquimod in human subjects induces a self-limited contact dermatitis–like reaction with signs of cytotoxicity and cell stress.**
- **This reaction is initiated by pDCs and shows a deviation toward the IL-23/T_H17 axis, the typical molecular signature of human psoriasis.**
- **The imiquimod model in human subjects represents a limited model of the molecular signature of psoriasis.**

REFERENCES

1. Lebwohl MG, Kavanaugh A, Armstrong AW, Van Voorhees AS. US perspectives in the management of psoriasis and psoriatic arthritis: patient and physician results from the population-based Multinational Assessment of Psoriasis and Psoriatic Arthritis (MAPP) Survey. Am J Clin Dermatol 2016;17:87-97.
2. Boehncke WH, Schon MP. Psoriasis. Lancet 2015;386:983-94.
3. Quaranta M, Knapp B, Garzorz N, Mattii M, Pullabhatla V, Pennino D, et al. Intraindividual genome expression analysis reveals a specific molecular signature of psoriasis and eczema. Sci Transl Med 2014;6:244ra90.
4. Suarez-Farinas M, Li K, Fuentes-Duculan J, Hayden K, Brodmerkel C, Krueger JG. Expanding the psoriasis disease profile: interrogation of the skin and serum of patients with moderate-to-severe psoriasis. J Invest Dermatol 2012;132:2552-64.
5. Swindell WR, Xing X, Stuart PE, Chen CS, Aphale A, Nair RP, et al. Heterogeneity of inflammatory and cytokine networks in chronic plaque psoriasis. PLoS One 2012;7:e34594.
6. Swindell WR, Sarkar MK, Liang Y, Xing X, Gudjonsson JE. Cross-disease transcriptomics: unique IL-17A signaling in psoriasis lesions and an autoimmune PBMC signature. J Invest Dermatol 2016;136:1820-30.
7. Tian S, Krueger JG, Li K, Jabbari A, Brodmerkel C, Lowes MA, et al. Meta-analysis derived (MAD) transcriptome of psoriasis defines the "core" pathogenesis of disease. PLoS One 2012;7:e44274.
8. Swindell WR, Johnston A, Carbajal S, Han G, Wohn C, Lu J, et al. Genome-wide expression profiling of five mouse models identifies similarities and differences with human psoriasis. PLoS One 2011;6:e18266.
9. Di Domizio J, Conrad C, Gilliet M. Xenotransplantation model of psoriasis. Methods Mol Biol 2017;1559:83-90.
10. Hawkes JE, Gudjonsson JE, Ward NL. The snowballing literature on imiquimod-induced skin inflammation in mice: a critical appraisal. J Invest Dermatol 2017;137:546-9.
11. van der Fits L, Mourits S, Voerman JS, Kant M, Boon L, Laman JD, et al. Imiquimod-induced psoriasis-like skin inflammation in mice is mediated via the IL-23/IL-17 axis. J Immunol 2009;182:5836-45.
12. Vinter H, Iversen L, Steiniche T, Kragballe K, Johansen C. Aldara(R)-induced skin inflammation: studies of patients with psoriasis. Br J Dermatol 2015;172:345-53.
13. Grine L, Dejager L, Libert C, Vandenbroucke RE. Dual inhibition of TNFR1 and IFNAR1 in imiquimod-induced psoriasiform skin inflammation in mice. J Immunol 2015;194:5094-102.
14. Dickson MC, Ludbrook VJ, Perry HC, Wilson PA, Garthside SJ, Binks MH. A model of skin inflammation in humans leads to a rapid and reproducible increase in the interferon response signature: a potential translational model for drug development. Inflamm Res 2015;64:171-83.
15. Singh TP, Zhang HH, Borek I, Wolf P, Hedrick MN, Singh SP, et al. Monocyte-derived inflammatory Langerhans cells and dermal dendritic cells mediate psoriasis-like inflammation. Nat Commun 2016;7:13581.
16. Yoshiki R, Kabashima K, Honda T, Nakamizo S, Sawada Y, Sugita K, et al. IL-23 from Langerhans cells is required for the development of imiquimod-induced psoriasis-like dermatitis by induction of IL-17A-producing gammadelta T cells. J Invest Dermatol 2014;134:1912-21.
17. Gilliet M, Conrad C, Geiges M, Cozzio A, Thurlimann W, Burg G, et al. Psoriasis triggered by toll-like receptor 7 agonist imiquimod in the presence of dermal plasmacytoid dendritic cell precursors. Arch Dermatol 2004;140:1490-5.
18. Lin Z, Yang C, Zhu Y, Duchi J, Fu Y, Wang Y, et al. Simultaneous dimension reduction and adjustment for confounding variation. Proc Natl Acad Sci U S A 2016;113:14662-7.
19. Gross CJ, Mishra R, Schneider KS, Medard G, Wettmarshausen J, Dittlein DC, et al. K+ efflux-independent NLRP3 inflammasome activation by small molecules targeting mitochondria. Immunity 2016;45:761-73.
20. Darsow U, Laifaoui J, Kerschenlohr K, Wollenberg A, Przybilla B, Wuthrich B, et al. The prevalence of positive reactions in the atopy patch test with aeroallergens and food allergens in subjects with atopic eczema: a European multicenter study. Allergy 2004;59:1318-25.
21. Eyerich S, Onken AT, Weidinger S, Franke A, Nasorri F, Pennino D, et al. Mutual antagonism of T cells causing psoriasis and atopic eczema. N Engl J Med 2011;365:231-8.
22. Eyerich K, Eyerich S, Biedermann T. The multi-modal immune pathogenesis of atopic eczema. Trends Immunol 2015;36:788-801.
23. Patel U, Mark NM, Machler BC, Levine VJ. Imiquimod 5% cream induced psoriasis: a case report, summary of the literature and mechanism. Br J Dermatol 2011;164:670-2.

24. Walter A, Schafer M, Cecconi V, Matter C, Urosevic-Maiwald M, Belloni B, et al. Aldara activates TLR7-independent immune defence. Nat Commun 2013;4:1560.
25. Eyerich K, Bockelmann R, Pommer AJ, Foerster S, Hofmeister H, Huss-Marp J, et al. Comparative in situ topoproteome analysis reveals differences in patch test-induced eczema: cytotoxicity-dominated nickel versus pleiotrope pollen reaction. Exp Dermatol 2010;19:511-7.
26. Traidl C, Sebastiani S, Albanesi C, Merk HF, Puddu P, Girolomoni G, et al. Disparate cytotoxic activity of nickel-specific CD8+ and CD4+ T cell subsets against keratinocytes. J Immunol 2000;165:3058-64.
27. Martin SF. Allergic contact dermatitis: xenoinflammation of the skin. Curr Opin Immunol 2012;24:720-9.
28. Kaplan DH, Igyarto BZ, Gaspari AA. Early immune events in the induction of allergic contact dermatitis. Nat Rev Immunol 2012;12:114-24.
29. Schmidt M, Raghavan B, Muller V, Vogl T, Fejer G, Tchaptchet S, et al. Crucial role for human Toll-like receptor 4 in the development of contact allergy to nickel. Nat Immunol 2010;11:814-9.
30. Lande R, Gregorio J, Facchinetti V, Chatterjee B, Wang YH, Homey B, et al. Plasmacytoid dendritic cells sense self-DNA coupled with antimicrobial peptide. Nature 2007;449:564-9.
31. Dombrowski Y, Peric M, Koglin S, Kammerbauer C, Goss C, Anz D, et al. Cytosolic DNA triggers inflammasome activation in keratinocytes in psoriatic lesions. Sci Transl Med 2011;3:82ra38.
32. Garzorz N, Krause L, Lauffer F, Atenhan A, Thomas J, Stark SP, et al. A novel molecular disease classifier for psoriasis and eczema. Exp Dermatol 2016;25:767-74.
33. El Malki K, Karbach SH, Huppert J, Zayoud M, Reissig S, Schuler R, et al. An alternative pathway of imiquimod-induced psoriasis-like skin inflammation in the absence of interleukin-17 receptor a signaling. J Invest Dermatol 2013;133:441-51.
34. Riol-Blanco L, Ordovas-Montanes J, Perro M, Naval E, Thiriot A, Alvarez D, et al. Nociceptive sensory neurons drive interleukin-23-mediated psoriasiform skin inflammation. Nature 2014;510:157-61.
35. Griffiths CE, Strober BE, van de Kerkhof P, Ho V, Fidelus-Gort R, Yeilding N, et al. Comparison of ustekinumab and etanercept for moderate-to-severe psoriasis. N Engl J Med 2010;362:118-28.
36. Gordon KB, Duffin KC, Bissonnette R, Prinz JC, Wasfi Y, Li S, et al. A phase 2 trial of guselkumab versus adalimumab for plaque psoriasis. N Engl J Med 2015;373:136-44.
37. Puig L. The role of IL-23 in the treatment of psoriasis. Expert Rev Clin Immunol 2017;13:525-34.

METHODS

Statistical analysis

For visual comparison of genes in respective pathways, absolute fold changes were plotted next to each other. Quantification was done by calculating the Pearson product-moment correlation coefficient between the fold changes of all genes in the pathways and its 95% CI.

Isolation of mouse pDCs

Immune cells from murine spleens and thymi were isolated by means of mechanical disruption of the organ, and single-cell suspensions were obtained by passing the cell solution through a nylon cell strainer. Bone marrow cells were isolated by flushing tibias and femurs with PBS. Cells of all organs were pooled, and erythrocytes were lysed. For isolation of pDCs, the Murine Plasmacytoid Dendritic Cell kit (Miltenyi Biotech) was used.

Double-staining immunohistochemistry

Tissue samples were fixed in 10% formalin solution and embedded in paraffin. Four-micrometer sections were cut. After deparaffinization and rehydration, epitope retrieval in boiling EDTA buffer (pH 8) was performed. Sections were incubated with the primary antibodies (rabbit anti-TLR7 [Abcam] and mouse anti-CD303 [Dendritics]) overnight at 4°C. The ZytoChem-Plus Double Stain Polymer-Kit, Permanent AP Red Kit, and Permanent HRP Green Kit (Zytomed Systems) were used to visualize TLR7 (anti-rabbit alkaline phosphatase polymer and alkaline phosphatase red chromogene)–bound and CD303 (anti-mouse HRP polymer and HRP green chromogen)–bound primary antibodies.

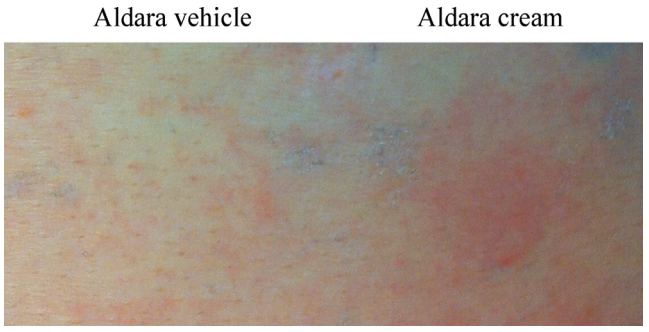

FIG E1. Application of Aldara vehicle not containing imiquimod does not induce ICD. Shown is a patient in whom Aldara and Aldara vehicle were patched occlusively over a period of 28 days twice weekly.

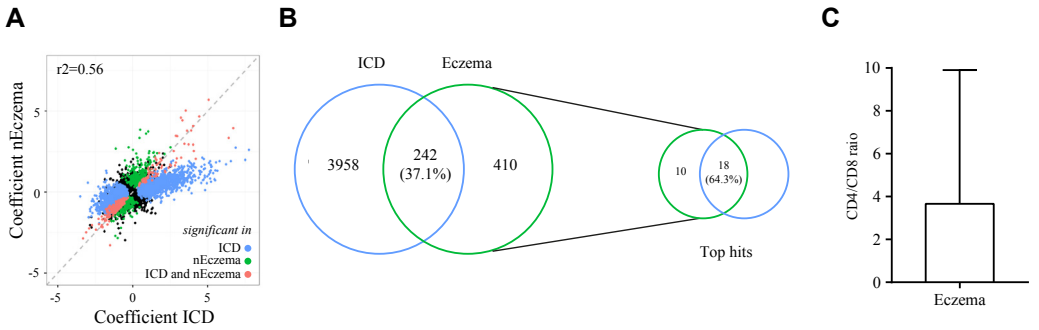

FIG E2. The ICD transcriptome does not correlate closely with atopic eczema. **A,** Correlation of all genes of ICD and eczema. Red, Genes significantly regulated in both lesions; green, genes regulated in patients with eczema; blue, genes regulated in patients with ICD; and black, not significantly regulated genes. **B,** Overlap of significantly regulated genes, as shown in Venn plots. Percentages indicate the relative number of genes regulated significantly in eczema that are also regulated significantly in patients with ICD. Smaller Venn plots indicate the overlap of top-hit genes with a $\log_2$ fold induction of greater than 2.5. **C,** CD4/CD8 ratio of eczema lesions (n = 15).

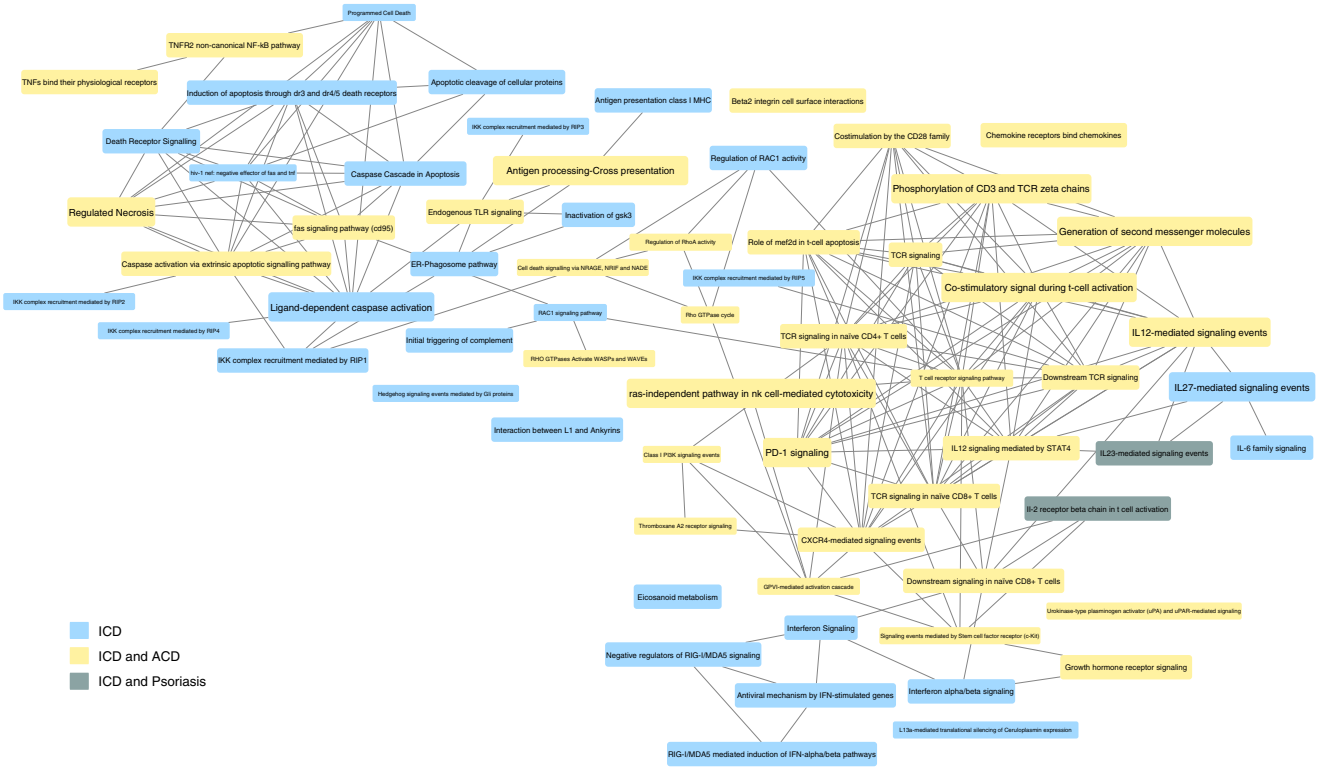

FIG E3. Comparative transcriptomic analysis of lesional ICD (n = 16), ACD (n = 10), and psoriasis (n = 24). Blue, Pathways regulated exclusively in patients with ICD; yellow, pathways regulated in patients with ICD and ACD; dark gray, pathways regulated in patients with ICD and psoriasis. Font size indicates the relative percentage of regulated genes within the pathway (small, 0% to 40% of all genes; medium, 40% to 60% of all genes; and large, >60%).

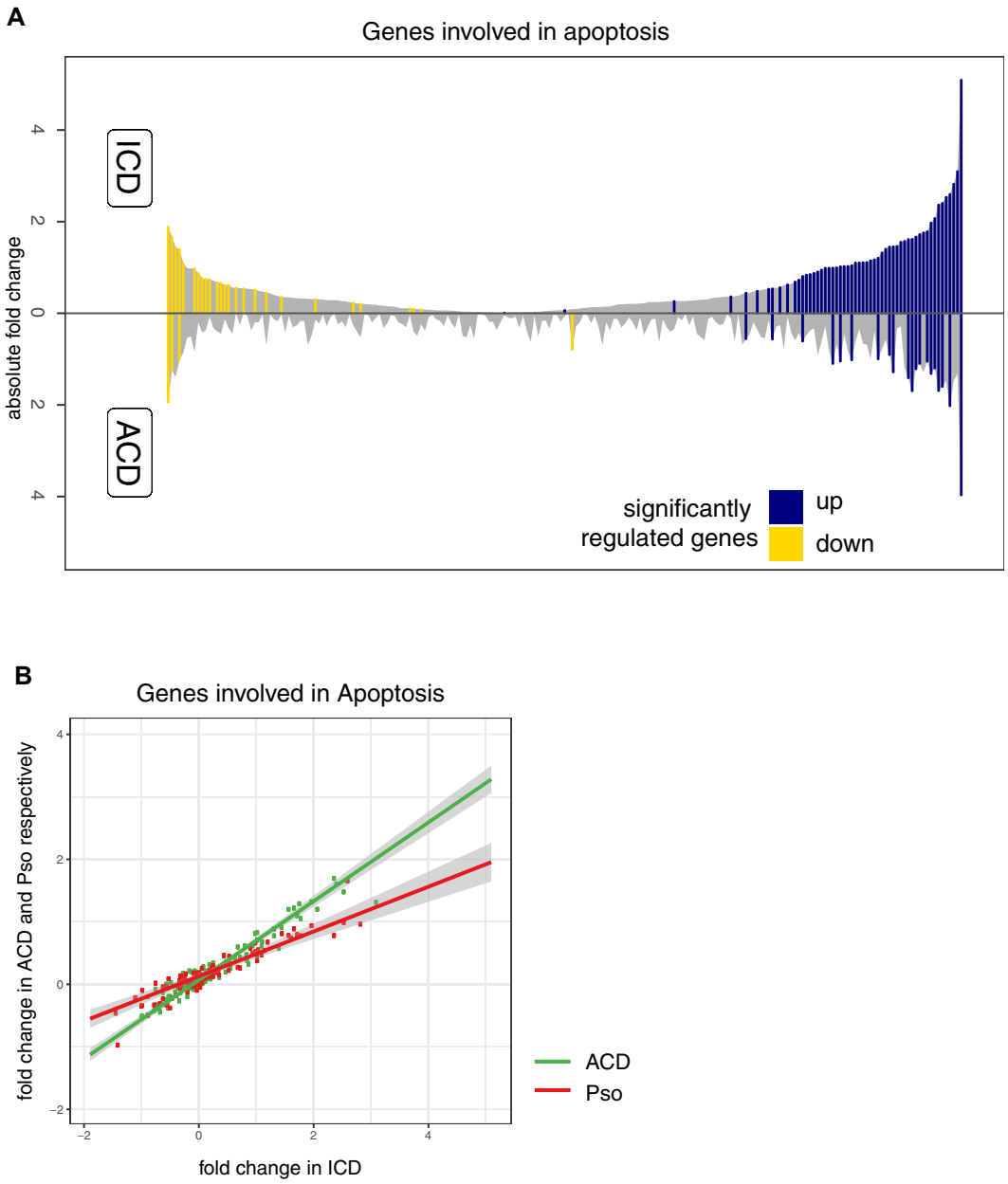

FIG E4. Differentially regulated genes within the pathway "apoptosis." **A,** Absolute fold change of each gene within the pathway "apoptosis" of the Reactome database in patients with ICD *(left)* and those with ACD *(right side)*, with significantly upregulated genes highlighted in blue and significantly downregulated genes highlighted in yellow. **B,** Correlation analysis of genes related to apoptosis. Shown are fold changes of genes in ICD lesions *(x-axis)* versus fold changes of genes in psoriasis (*y-axis*, *red dots* and *line*) or ACD (*y-axis*, *green dots* and *line*) lesions. *Lines* indicate degree of correlation.

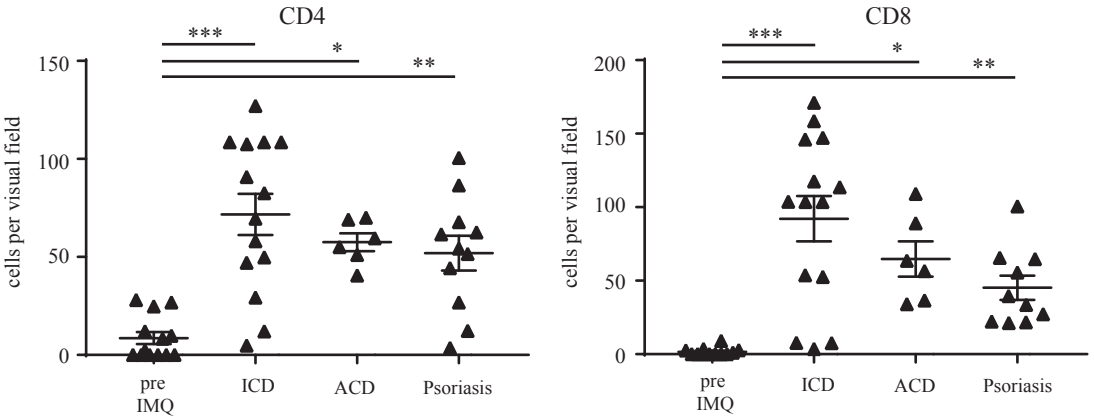

FIG E5. *In situ* expression of $CD4^+$ and $CD8^+$ T cells in patients with ICD, ACD, and psoriasis. Quantitative analysis of $CD4^+$ and $CD8^+$ cells in immunohistochemical staining. Shown are means ± SEMs, and each *symbol* represents 1 sample. $*P < .05$, $**P < .01$, and $***P < .001$.

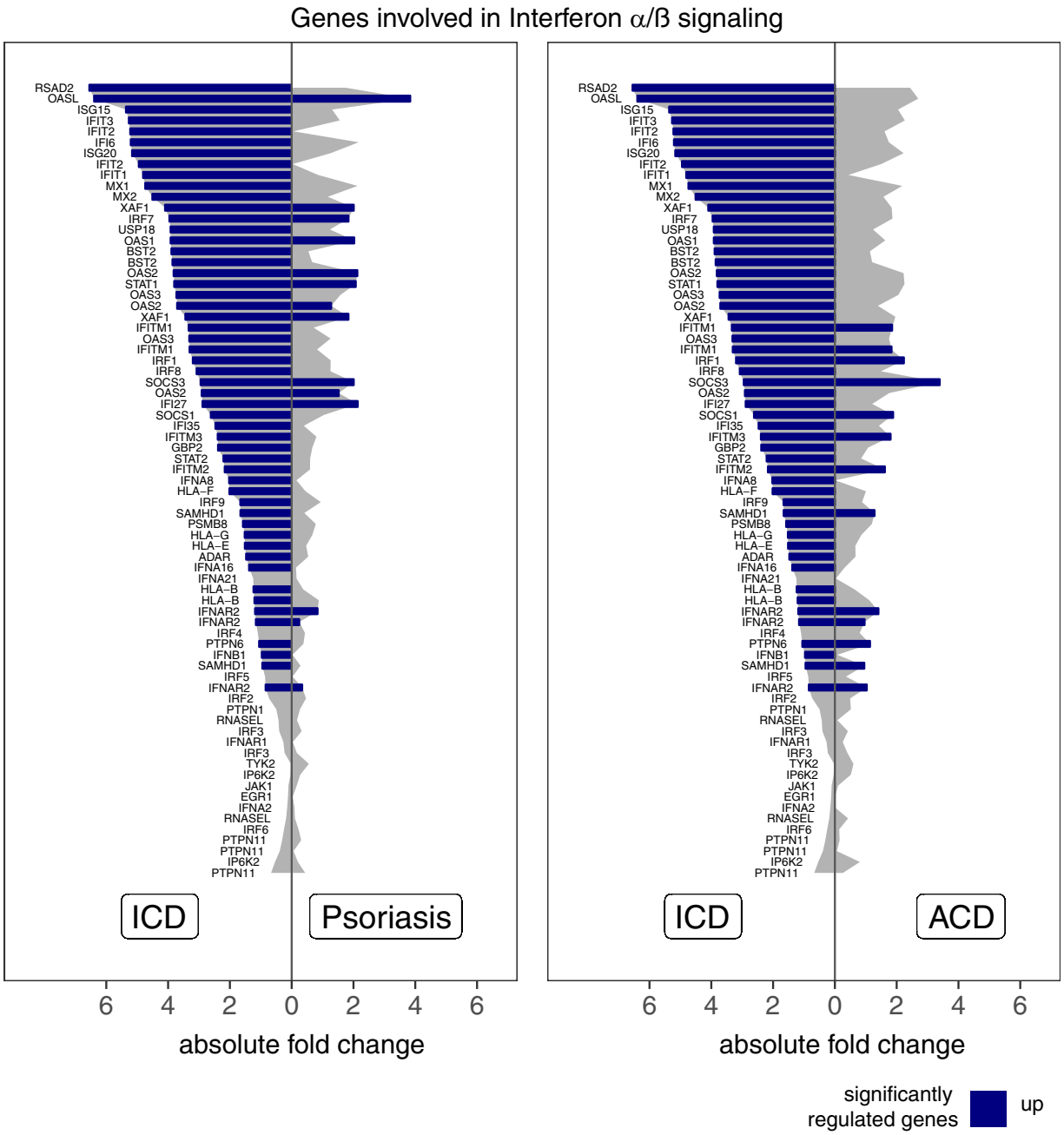

FIG E6. Differentially regulated genes from the pathway "IFN-α/β signaling." Shown is the absolute fold change of each gene within the pathway "IFN-α/β signaling" of the Reactome database in comparison of patients with ICD and psoriasis *(left)* and patients with ICD and ACD *(right)*, with significantly upregulated genes highlighted in blue.

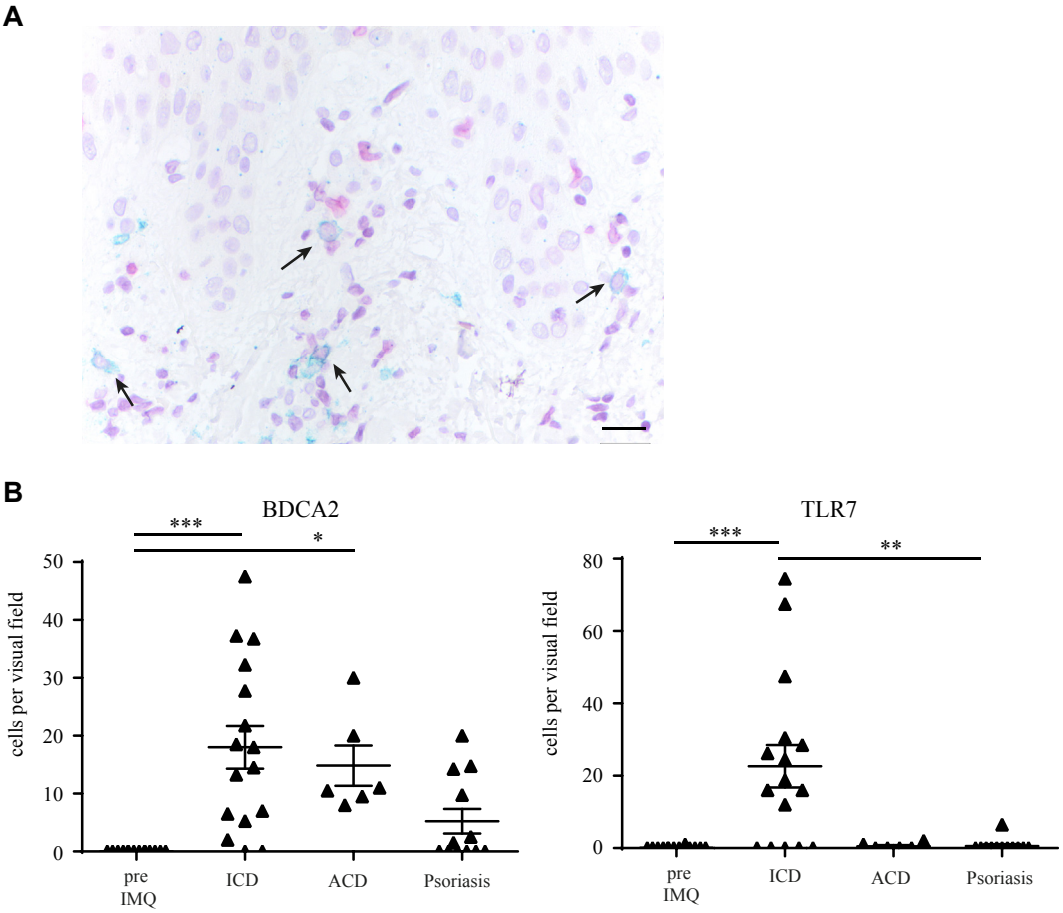

FIG E7. BDCA2$^+$TLR7$^+$ cells in patients with ACD and those with psoriasis. **A,** Double immunohistochemistry labeling of BDCA2 (green) and TLR7 (red) indicates double-positive pDCs in patients with ICD. Shown is one representative staining. *Bar* = 20 μm. **B,** Quantitative analysis of CD4$^+$ and CD8$^+$ cells in immunohistochemical staining. Shown are means ± SEMs, and each *symbol* represents 1 sample. **P* < .05, ***P* < .01, and ****P* < .001.

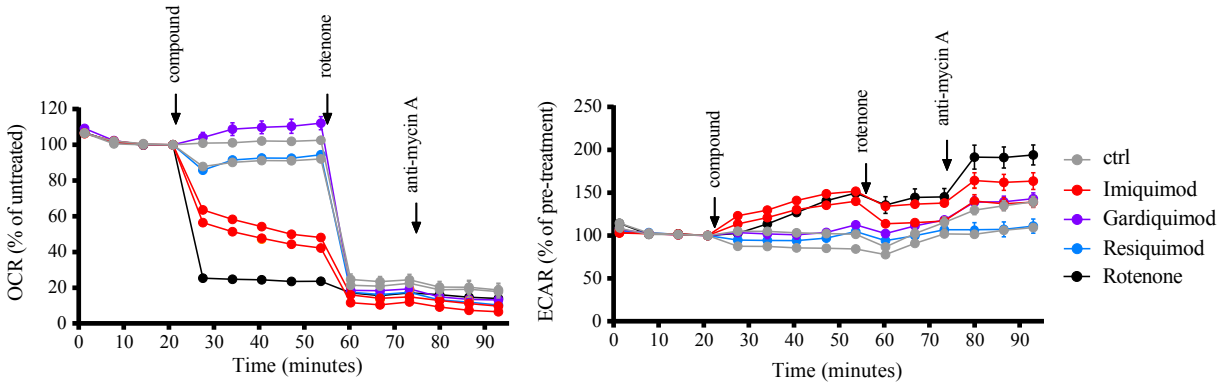

FIG E8. Extracellular flux analysis of murine pDCs. Oxygen consumption rate (*OCR*, *left graph*) and extracellular acidification *(ECAR)* of primary human pDCs stimulated with imiquimod *(IMQ)*, R848, or gardiquimod *(GAR)* over time compared with unstimulated pDCs. *Arrows* indicate addition of compound or rotenone application.

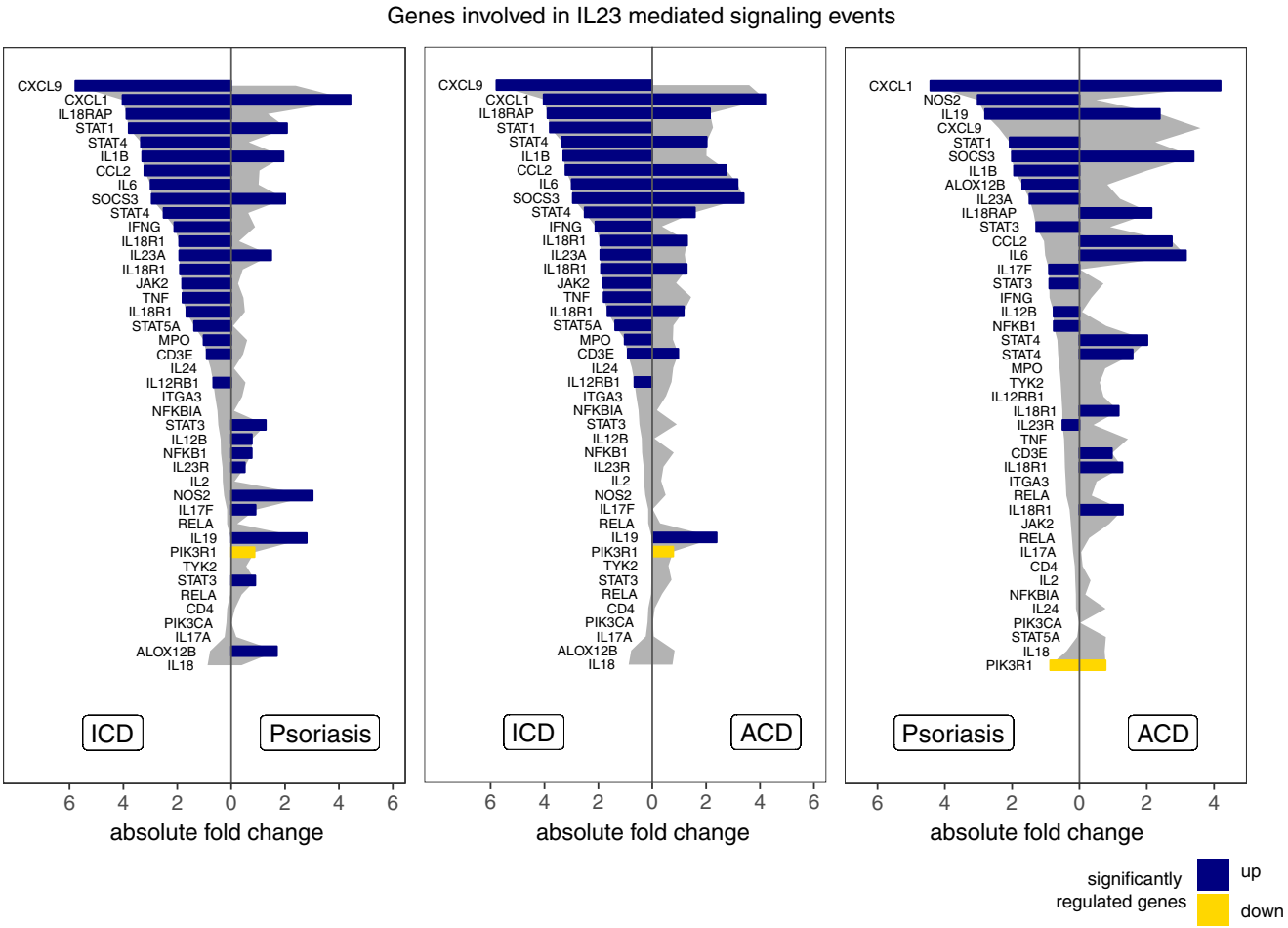

FIG E9. Differentially regulated genes from the IL-23 pathway. Shown is the absolute fold change of each gene within the pathway "IL-23 signaling" of the Reactome database in comparison of patients with ICD and psoriasis *(left)*, patients with ICD and ACD *(middle)*, and patients with psoriasis and ACD *(right)*, with significantly upregulated genes highlighted in blue and significantly downregulated genes highlighted in yellow.

TABLE E1. Pathways regulated in patients with ICD, ACD, and psoriasis

Pathway	Set size	Candidates contained	*P* value	q value
IL-23–mediated signaling events	37 (37)	18 (48.6%)	.000111	0.00172
IL-12–mediated signaling events	64 (58)	36 (62.1%)	5.11e-12	4.92e-10
Antigen processing, cross-presentation	49 (43)	29 (67.4%)	3.05e-11	2.45e-09
Generation of second messenger molecules	38 (26)	19 (73.1%)	1.05e-08	6.31e-07
TCR signaling	69 (55)	29 (52.7%)	1.04e-07	5.56e-06
PD-1 signaling	28 (18)	14 (77.8%)	2.74e-07	1.32e-05
Ligand-dependent caspase activation	17 (16)	13 (81.2%)	3.06e-07	1.34e-05
TCR signaling in naive $CD8^+$ T cells	56 (50)	26 (52.0%)	6.78e-07	2.72e-05
Phosphorylation of CD3 and TCR-ζ chains	27 (17)	13 (76.5%)	1.06e-06	3.91e-05
TCR signaling in naive $CD4^+$ T cells	70 (63)	29 (46.0%)	3.97e-06	0.00012
Regulated necrosis	16 (16)	12 (75.0%)	4.00E-06	0.00012
Chemokine receptors bind chemokines	50 (45)	23 (51.1%)	4.38e-06	0.000124
IL-27–mediated signaling events	26 (26)	16 (61.5%)	5.5e-06	0.00014
CXCR4-mediated signaling events	88 (80)	34 (42.5%)	5.53e-06	0.00014
Caspase cascade in apoptosis	57 (55)	26 (47.3%)	6.8e-06	0.000164
Interferon signaling	71 (56)	26 (46.4%)	1.03e-05	0.000234
TNFR2 noncanonical NF-κB pathway	52 (47)	23 (48.9%)	1.12e-05	0.000234
Caspase activation through extrinsic apoptotic signaling pathway	28 (26)	15 (57.7%)	3.23e-05	0.000648
Costimulatory signal during T-cell activation	21 (16)	11 (68.8%)	3.88e-05	0.000746
Programmed cell death	125 (119)	43 (36.1%)	4.66e-05	0.000862
Downstream signaling in naive $CD8^+$ T cells	68 (57)	25 (43.9%)	5.01e-05	0.000892
IL-12 signaling mediated by STAT4	32 (28)	15 (53.6%)	.000103	0.00166
Costimulation by the CD28 family	75 (63)	26 (41.3%)	.000124	0.0018
ER-phagosome pathway	24 (23)	13 (56.5%)	.000147	0.00196
Negative regulators of RIG-I/MDA5 signaling	25 (23)	13 (56.5%)	.000147	0.00196
Induction of apoptosis through dr3 and dr4/5 death receptors	23 (23)	13 (56.5%)	.000147	0.00196
Endogenous TLR signaling	27 (24)	13 (54.2%)	.000261	0.0033
Ras-independent pathway in NK cell–mediated cytotoxicity	22 (16)	10 (62.5%)	.000289	0.00356
IFN-α/β signaling	27 (19)	11 (57.9%)	.000364	0.00418
RIG-I/MDA5–mediated induction of IFN-α/β pathways	57 (53)	22 (41.5%)	.000365	0.00418
Apoptotic cleavage of cellular proteins	39 (37)	17 (45.9%)	.000406	0.00455
Fas signaling pathway (CD95)	20 (20)	11 (55.0%)	.000661	0.00723
IL-6 family signaling	27 (26)	13 (50.0%)	.00072	0.00753
TNFs bind their physiologic receptors	30 (26)	13 (50.0%)	.00072	0.00753
Growth hormone receptor signaling	19 (18)	10 (55.6%)	.00106	0.0106
Antigen presentation: folding, assembly, and peptide loading of class I MHC	24 (21)	11 (52.4%)	.00113	0.0111
HIV-1 Nef: negative effector of Fas and TNF	53 (51)	20 (39.2%)	.00156	0.015
Rho GTPase cycle	145 (130)	41 (31.5%)	.00172	0.0162
Initial triggering of complement	104 (19)	10 (52.6%)	.00182	0.0165
Eicosanoid metabolism	23 (22)	11 (50.0%)	.00185	0.0165
Regulation of RAC1 activity	39 (35)	15 (42.9%)	.0021	0.0181
Death receptor signaling	44 (42)	17 (40.5%)	.0023	0.0194
Hedgehog-signaling events mediated by GLI proteins	50 (46)	18 (39.1%)	.0027	0.022
IKK complex recruitment mediated by RIP1	26 (23)	11 (47.8%)	.0029	0.0232
Downstream TCR signaling	48 (36)	15 (41.7%)	.00294	0.0232
Class I PI3K signaling events	46 (43)	17 (39.5%)	.00309	0.024
Thromboxane A_2 receptor signaling	57 (51)	19 (37.3%)	.00399	0.029
β_2-Integrin cell-surface interactions	30 (27)	12 (44.4%)	.00403	0.029
Interaction between L1 and ankyrins	30 (27)	12 (44.4%)	.00403	0.029
RAC1 signaling pathway	54 (52)	19 (36.5%)	.00511	0.0356
GPVI-mediated activation cascade	54 (52)	19 (36.5%)	.00511	0.0356
Antiviral mechanism by interferon-stimulated genes	34 (28)	12 (42.9%)	.00577	0.0391
Urokinase-type plasminogen activator (uPA) and uPA receptor–mediated signaling	43 (42)	16 (38.1%)	.0062	0.0414
Role of MEF2D in T-cell apoptosis	31 (25)	11 (44.0%)	.0064	0.0422
Inactivation of GSK3 by Akt causes accumulation of β-catenin in alveolar macrophages	42 (39)	15 (38.5%)	.00717	0.046
Signaling events mediated by stem cell factor receptor (c-Kit)	52 (50)	18 (36.0%)	.00756	0.0472
T-cell receptor signaling pathway	55 (50)	18 (36.0%)	.00756	0.0472
Regulation of RhoA activity	49 (43)	16 (37.2%)	.00804	0.0496
RHO GTPases Activate WASPs and WAVEs	37 (36)	14 (38.9%)	.00828	0.0504
IL-2 receptor β-chain in T-cell activation	48 (47)	17 (36.2%)	.00882	0.0519
L13a-mediated translational silencing of ceruloplasmin expression	129 (97)	30 (30.9%)	.00907	0.0519
Cell death signaling through NRAGE, NRIF, and NADE	78 (70)	23 (32.9%)	.0097	0.0549

ER, Endoplasmic reticulum; *GLI*, proteins of the Gli family; *GPVI*, glycoprotein VI; *GSK3*, glykogensynthase-kinase 3; *IKK*, IκB kinase; *MEF2D*, myocyte enhancer factor 2D; *NADE*, NH(3)-dependent NAD(+) synthetase; *NF-κB*, nuclear factor κB; *NK*, natural killer; *NRAGE*, melanoma-associated antigen D1; *NRIF*, neurotrophin receptor interacting factor; *PD-1*, programmed death protein 1; *PI3K*, phosphoinositide 3-kinase; *RAC1*, Ras-related C3 botulinum toxin substrate 1; *RIG-I/MDA5*, retinoic acid inducible gene I/melanoma differentiation antigen 5; *RIP1*, Rieske iron-sulfur protein; *STAT4*, signal transducer and activator of transcription 4; *TCR*, T-cell receptor; *TNFR2*, tumor necrosis factor receptor 2; *WASP*, Wiskott -Aldrich syndrome protein; *WAVE*, WASP-family verprolin-homologous protein.